MINERAL CHARACTERIZATION AND CATALOGING OF QUARRIED AGGREGATE SOURCES USED IN MICHIGAN HIGHWAY CONSTRUCTION

Volume I: Final Report

Submitted to the

Michigan Department of Transportation

By

Lawrence Sutter, Ph.D.
Principal Investigator
Transportation Materials Research Center
Michigan Technological University
Dept. of Civil and Environmental Engineering
1400 Townsend Drive
Houghton, MI 49931

Thomas Van Dam, Ph.D., P.E.
Co-Principal Investigator
Transportation Materials Research Center
Michigan Technological University

Karl Peterson
Co-Principal Investigator
Transportation Materials Research Center
Michigan Technological University

January 2005

TABLE OF CONTENTS

LIST OF FIGURES

LIST OF TABLES

CHAPTER 1 - INTRODUCTION

The physical and chemical properties of quarried aggregates play an important role in determining their suitability for use in portland cement concrete (PCC). Mechanical strength, coefficient of thermal expansion, possible chemical reactivity, and soundness are a few aggregate properties that significantly affect the long-term performance and durability of portland cement concrete pavements (PCCP). The effect of aggregate properties on concrete durability has been, and continues to be, the topic of much research. Ultimately, to integrate knowledge about aggregate properties into modern construction practices, it is necessary that Michigan's quarried aggregate sources be characterized and cataloged in an easily accessible database for easy reference by engineers, technicians, or others involved in the production of high quality PCC for Michigan roads. As a result, the Michigan Department of Transportation (MDOT) initiated this study to better understand and catalog key chemical and physical properties of quarried aggregates used in the production of PCCP in Michigan, with the ultimate goal of creating a user-friendly reference database.

Project Objectives

The project objectives were:

- Perform a mineralogical characterization of Michigan's principal quarried aggregate sources used in PCCP.

- Establish a user-friendly database with pertinent mineralogical information on Michigan's principal quarried aggregate sources used in PCCP.

- Compare the mineralogical characteristics of Michigan's quarried aggregate sources with known deleterious characteristics of aggregates as identified in the literature.

Research Plan

To achieve the project objectives, a number of tasks were undertaken. First, a literature review was performed of publications discussing aggregate reactivity and soundness for concrete in a wet-freeze environment and subjected to common deicing chemicals. This literature review is included in the background presented in Chapter 2 of this final report. Then, in cooperation with MDOT, 13 quarried aggregate sources used in Michigan PCCP were sampled. Within each source, different aggregate types were identified by visual characteristics. The samples obtained were hand samples from pit production material. Additionally, stockpiles of 6AA were sampled for physical property determination.

The specimens were analyzed in laboratories at MTU, the University of Michigan (U of M), and at the Calcite Quarry in Rogers City, Michigan. At MTU petrographic analysis was performed on polished slabs and thin sections produced from larger pieces of aggregate sampled from each source. Mineralogy, grain size, porosity, and chemical composition were determined using, as appropriate, optical microscopy, scanning electron microscopy, x-ray microanalysis, x-ray microscopy, and x-ray diffraction. In addition, specimens were sent to the U of M for coefficient of thermal expansion (CTE) determination. Bulk composition was determined by x-ray fluorescence spectrometry at the Calcite Quarry, Rogers City, Michigan. The resulting data was summarized into easily updated portfolio documents of each quarry, available for access and download on the worldwide web (WWW). Additionally, the aggregate characteristics of the sources in this study are compared to characteristics of durable and non-durable aggregates published in the literature.

CHAPTER 2 - BACKGROUND

Production of durable PCCP requires raw materials that meet the design requirements of the pavement concrete mixture and are suitable for the environment in which the concrete is placed. Additionally, the materials used in the concrete must be able to coexist in the concrete mixture without adverse chemical and physical interactions that may result in distress. Given that coarse aggregate occupies 60 - 75% of the concrete by volume, its properties greatly influence the design characteristics and durability of the concrete.

Distress in PCCP can result from a number of sources. One potential problem arises if the characteristics of the coarse aggregates used in mixture production differ from those assumed during pavement design. For example, in the new AASHTO 2002 concrete pavement design procedures, the concrete coefficient of thermal expansion (CTE_{PCC}) is a required design input parameter. The CTE_{agg} is largely related to the CTE of the coarse aggregate and to a lesser extent the CTE of the fine aggregate. Most empirical formulae to estimate CTE of concrete consider the volume and CTE of aggregate and the volume and CTE of cement paste, and do not separate the fine from coarse aggregate (http://www.hiperpav.com/theory3.asp). Using an aggregate possessing significantly different CTE properties as compared to that assumed in design may lead to distress in the pavement. Concrete distress resulting from such occurrences can be generally referred to as design related distress. Another source of distress can result from adverse interactions between the concrete components and/or it's environment. This type of distress is called materials related distress (MRD). Both of these general categories will be discussed as they pertain to aggregates and their specification for use in concrete.

Design Related Distress

Of the physical properties affecting the performance of coarse aggregate in a concrete mixture, the coefficient of thermal expansion may be one of the most important. For pavements, the value of a concrete's coefficient of thermal expansion (CTE$_{PCC}$) is considered very important in computing joint movement and slab curling stress development (PCA, 1988). Given that joint load transfer decreases with increasing joint opening, an accurate estimate of the joint opening is essential in evaluating performance. According to Darter and Barenberg (1977), the relationship between joint opening and change in temperature can be written as:

$$\Delta L = C \cdot L \left(CTE_{PCC} \cdot \Delta T + \varepsilon \right)$$

(2-1)

where ΔL = joint opening (mm).

C = adjustment factor for slab-subbase friction.

L = slab length (mm).

ΔT = maximum temperature range (temperature at placement/setting time minus lowest mean monthly temperature) (ϒC).

CTE$_{PCC}$= PCC coefficient of thermal expansion (/ϒC).

ε = PCC shrinkage coefficient (mm/mm).Slab curling stress can be a significant contributor to fatigue cracking for bottom-up as well as top-down cracking. The traditional type of fatigue cracking is initiated at the bottom of the slab, and these can be transverse cracks initiated at the midslab edges, and longitudinal cracks initiated in the wheel paths at transverse joints (Huang, 1993). Top-down fatigue cracking can be initiated if the slab is subjected to large repeated tensile stresses at the top of the slab.

These stress conditions can occur if the slab has a predominantly upward concave shape from curling and warping and/or if the slab experiences loss of support at the joints, causing high tensile stresses from corner loading. (e.g. Teller and Bosley, 1930; Teller and Sutherland, 1935; Rhodes, 1949; Poblete et al., 1991; Poblete et al., 1989; Hansen et al., 1998; and Titus-Glover et al., 1999). Recent research has demonstrated that temperature curling associated with the daily and seasonal temperature fluctuations can cause significant loss of joint support and associated slab cracking (Hansen et al., in press).

Slab curling is caused by the temperature differential that commonly exists between the top and bottom of the slab. This differential changes constantly as rapid changes in surface temperature occur throughout the day as the amount of solar radiation changes. As the slab curls, stress is generated as the self-weight of the concrete resists the lifting of the slab. Equation (2-2) below demonstrates how the curling stresses depend on several factors including the CTE_{PCC}:

$$\sigma_{x(y)} = \frac{E \cdot CTE_{PCC} \cdot \Delta T}{2(1-\upsilon^2)} \left(C_{x(y)} + \upsilon C_{y(x)} \right)$$

(2-2)

where $\sigma_{x(y)}$ = stress in the x or y direction (MPa).

E= PCC elastic modulus (MPa)

ν= PCC Poisson's ratio

ΔT = temperature differential between the top and the bottom of the slab (ΥC).

C = correction factor for slab geometry in terms of ratio of slab length, L, to radius of relative stiffness, l. This factor increases from zero to 1.1 with increasing slab length.

The CTE_{PCC} is highly dependent on the mix composition (e.g., Neville, 1997; Addis, 1986; and Van Dam, 1995) and is determined by the coefficient of thermal expansion of the cement paste (CTE_{ce}) and that of the aggregates (CTE_{agg}). Aggregate type has a significant influence on the CTE_{PCC} due to the high volume content of coarse and fine aggregate in concrete (Zoldners, 1971). The cement paste and the aggregate have different CTE values (Neville, 1997). The CTE_{ce} (hydrated cement paste) varies between 11 to 20 x $10^{-6}/°C$, which can be substantially higher than the CTE_{agg}. Typical CTE_{agg} values of different rock types, as reported by Lane (1994), are shown in Table 2-1.

Table 2-1 Typical CTE_{agg} values of different rock types. [after Lane (1994)]

Rock	CTE_{agg} value (x$10^{-6}/°C$)
Quartzite, silica shale, chert	11.0-12.5
Sandstones	10.5-12.0
Quartz sands and pebbles	10.0-12.5
Argillaceous shales	9.5-11.0
Dolomite, magnesite	7.0-10.0
Granite, gneiss	6.5-8.5
Syenite, andesite, diorite, phonolite, gabbro, diabase, basalt	5.5-8.0
Marble	4.0-7.0
Dense, crystalline, porous limestone	3.5-6.0

Materials Related Distress

Materials-related distress refers to concrete pavement distress that is directly the result of the properties of the materials used and their interaction with each other and the environment in which it is placed. These failures are differentiated from others that may be most closely associated with inadequate design, improper construction, or traffic loading of the pavement. The occurrence of MRD in a PCCP is a function of many factors, including the constituent materials used (e.g. aggregate, cement, and admixtures),

the climatic conditions to which it is subjected, and the presence of external agents such as deicing chemicals or sulfates.

MRDs generally appear on the pavement surface as fine cracking or as a material degradation such as scaling or spalling. The distress may occur only in the vicinity of joints or cracks (e.g. aggregate freeze-thaw deterioration) or it may be distributed over the pavement surface (e.g. alkali-aggregate reaction). Discoloration of the concrete, sometimes referred to as staining, is also a common feature. In some instances, concrete expansion may occur, resulting in blowups at joints and displacement of fixed structures. These distresses may occur as soon as a few years after construction.

In general, the development of MRD can be attributed to either physical or chemical mechanisms, although the two often act together to initiate and propagate distress. Three causes of concrete deterioration that are related to the coarse aggregate fraction are aggregate freeze-thaw deterioration (commonly known as D-cracking), deterioration by alkali-aggregate reactions, and deterioration by deicing salts. Fine aggregates are not associated with aggregate-related F-T deterioration due to their small size but can deteriorate by alkali-aggregate reactions. The role of fine aggregate in deicer distress, if any, is not discussed in the literature.

Aggregate Freeze-Thaw Deterioration

Freeze-thaw deterioration of aggregate is associated with the freezing and thawing of susceptible, coarse aggregate particles in the concrete. The resulting pavement distress is commonly referred to as D-cracking. There are multiple theories on how this distress occurs. In one theory, aggregates identified as being D-cracking susceptible either fracture as they freeze or dilate significantly, resulting in cracking of the surrounding

mortar. Another theory holds that D-cracking susceptible aggregates allow for rapid expulsion of water during freezing contributing to dissolution of soluble paste components at the aggregate-paste interface. Regardless of the mechanism, the key aggregate properties related to D-cracking susceptibility are aggregate size, pore size distribution, and strength (Mindess and Young 1981). Most D-cracking susceptible aggregates are of sedimentary origin (e.g., cherts, sandstones, shales, and limestones), can be calcareous or siliceous, and can be gravel or crushed rock (Neville 1996).

As stated, there are two different mechanisms that are associated with aggregate related F-T damage, including damage to the aggregates themselves and/or damage to the adjacent paste system. Powers' hydraulic pressure theory is generally considered to provide a reasonable description of the actions taking place inside aggregate particles during freezing (Pigeon 1995). Given a critically saturated aggregate, excessive pressures can develop due to the volume increase associated with ice formation. The expansion associated with ice formation may be accommodated by either elastic deformation and / or the expulsion of unfrozen water. If an aggregate is less than critically saturated, or can expel water to its surroundings, internal hydraulic pressures result as unfrozen water is forcibly displaced by ice formation. The hydraulic pressures are greater when this flow is through smaller sized pores and along longer flow paths (Winslow 1994). The tensile capacity of an aggregate can be exceeded when either the expansion due to ice formation cannot be accommodated by elastic deformation or the hydraulic pressures become excessive. In other cases, the expulsion of water from sound aggregate particles during a freezing event can result in damage to the surrounding paste phase.

It is fairly well established that the aggregate pore system is the most important factor contributing to its F-T durability (Schwartz 1987, Winslow 1994, Pigeon 1995). Two related elements of the pore system that are of particular interest are the porosity and pore size distribution. Aggregate porosity is the ratio of the surface accessible pore volume to the total aggregate volume. Porosity is a characteristic that is relatively straightforward to determine and provides a measure of the total volume of water that can be contained within a fully saturated aggregate. Pore size is a measure of the physical dimensions of the various elements of the accessible pore volume. It is a much more difficult characteristic to determine, but provides an important indication of an aggregate's potential to become critically saturated and is also a measure of its permeability or resistance to fluid flow during a freezing event.

Perhaps the single most significant pore characteristic is the volume of the total porosity contained within a range of pore sizes that have been empirically related to aggregate F-T durability (Kaneuji 1980). In this work, the authors developed a relationship between the median pore diameter (MD) and the pore volume coarser than 0.0045 μm (PV) with the expected durability factor (EDF) obtained from performing ASTM C 666 *Standard Test Method for Resistance of Concrete to Rapid Freezing and Thawing*. The relationship they established is presented in equation 2-3. The authors state that any aggregate with an EDF < 40 is freeze-thaw susceptible.

$$EDF = 0.579/PV + 6.12MD + 3.04 \qquad\qquad (2\text{-}3)$$

The exact limit of detrimental pore sizes is not definitively established, but has been reported to be in the range of under 0.005 μm up to 5 μm (Kaneuji 1980, Marks 1982, Shakkor 1982). Marks and Dubberke (1982) have done research focusing on the pore

system of limestones used as coarse aggregate in concrete, and the relationship between it and D-cracking. They found that most F-T reactive aggregates have pore sizes with radii ranging from 0.04 - 0.2 μm. Parts of the pore system smaller than the lower limit are not considered detrimental for one of two reasons. Either their size is such that the water in them will not freeze at normal winter temperatures or the contained volume of water is small enough that it does not contribute significantly to stresses in either the aggregate itself or the surrounding paste. Pore systems with sizes greater than the upper limit are not considered detrimental to the aggregate because either they do not become critically saturated or their permeability is high enough that they do not generate excessive hydraulic pressures. Aggregates with a preponderance of pore sizes within the detrimental size range are believed to have a higher potential to become critically saturated and/or develop excessive hydraulic pressures due to low permeability.

Kaneuji (1980) also argues that it is the combination of pore size and pore volume that is important as more porous aggregates can easily become critically saturated. Therefore, the relationship given in equation 2-3 is a function of both pore size and pore diameter.

Because internal hydraulic pressures are directly proportional to the length of the flow path, reducing the size of the aggregate can reduce the magnitude of these internal pressures. Reducing the aggregate size can also result in a smaller volume of expelled water per unit surface area. Experimental studies have confirmed an increased F-T durability of susceptible aggregates with a reduction in maximum particle size (Stark 1973). The maximum particle size to ensure a F-T durable aggregate varies greatly because it depends on the characteristics of the aggregate pore system including the

porosity and the pore size distribution (which will affect the degree of saturation and permeability), along with the mechanical properties of the aggregate. Additionally, the properties of the surrounding paste system influences the value of this maximum size.

While reducing the maximum particle size may improve the F-T performance of some aggregates, it also typically results in an increased cement paste/mortar volume. In addition to being more expensive, a higher paste volume can increase drying shrinkage and result in reduced aggregate interlock at joints and across structural cracks. It also will increase the total alkalinity per unit volume of concrete and thus may contribute to alkali-aggregate reactivity (Leming 1996).

Freeze-thaw deterioration can be identified by combined field and laboratory analysis as summarized in recent publications (Van Dam 2002a, Van Dam 2002b, Sutter 2002). In the field, aggregate freeze-thaw deterioration of concrete is initially visible as a series of fine cracks generally running parallel to joints, cracks, or free edges in the slab. The deterioration commonly starts near the bottom of the concrete slab where excess moisture accumulates and as cracks form, they propagate to the surface. Increased permeability results from this cracking and from the leaching of calcium hydroxide from the cement paste by fluids permeating the cracked concrete. As the number of freeze-thaw cycles increases, spalling and deterioration of the cracks will occur. A dark staining due to calcium hydroxide or calcium carbonate residue generally precedes and accompanies the cracking, often in an hourglass shape on the pavement surface at affected joints and cracks.

In the laboratory using a stereo optical microscope (SOM) or a petrographic optical microscope (POM), diagnostic features of aggregate FT can be observed. Cracks

through non-reactive coarse aggregates are very typical of aggregate FT but care must be exercised in rushing to judgment as cracks are also common in the case of alkali–aggregate reaction. Gaps between the aggregate and paste form. These gaps may result from the dissolution of calcium hydroxide at the aggregate/paste interface or coarse aggregate dilation due to freezing. Subsequent re-deposition of calcium hydroxide or calcite may occur in the cracks. As previously discussed, as a percentage of the total aggregate void space, excessive amounts of voids in the aggregate with diameters less than 5 microns is thought to be detrimental to aggregate freeze-thaw resistance.

Alkali-Aggregate Reactions

<u>Alkali-Carbonate Reaction</u>

Various chemical reactions involving coarse aggregate, cement paste, and concrete pore water occur with some being deleterious. One such deleterious reaction is the alkali-carbonate reaction (ACR), which occurs between carbonate aggregates and pore fluids in the concrete. In general, ACR is the conversion of dolomite to limestone by chemical reactions between the concrete pore fluids and dolomite coarse aggregate where magnesium (Mg^{2+}) in the dolomite mineral structure is replaced with calcium (Ca^{2+}) from the pore fluid. This process results in volume changes in the concrete from the production of reaction products and disintegration of aggregates, which further results in concrete distress. A simple dedolomitization reaction is shown below in equation 2-4.

$$CaMg(CO3)_2 + Ca^{2+} \rightarrow 2CaCO_3 + Mg^{2+} \qquad (2\text{-}4)$$
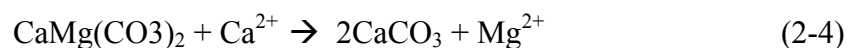
In equation 2-4, calcium ions are supplied by the concrete pore water, which is rich in many dissolved species. In addition to reactions with calcium hydroxides, dolomite can

and does chemically react with alkali metal hydroxides. The widely accepted chemical reaction between dolomite and alkali metal hydroxides is given in equation 2-5 and results in a reported 5% decrease in volume (Cody et al., 1994).

$$CaMg(CO3)_2 + 2OH^- \rightarrow CaCO_3 + Mg(OH)_2 + CO_3^{2-} \qquad (2\text{-}5)$$
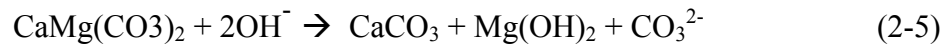
In this reaction dolomite reacts with alkali derived from the high pH of concrete pore water resulting in the formation of brucite ($Mg(OH)_2$), calcite ($CaCO_3$), and carbonate ions (CO_3^{2-}). The pore solution of concrete is an alkaline solution, primarily a result of the sodium and potassium ions released during cement hydration. Excess alkalis are also derived from admixtures, mixing water, fly ash, ground granulated blast furnace slag, silica fume, and external sources (CCAA 1996). The type of aggregate susceptible to this type of reaction in the alkaline solution is typically a fine-grained matrix of calcite and clay that suspends larger crystals of dolomite (Ozol 1994). ACR requires a source of moisture in order to have deleterious consequences.

The mechanisms presented previously is a simplified description of the actual mechanism as the expansion portion of the reaction is still being debated. There are two main theories on how the expansion of the concrete occurs. The first theory suggests that expansion is caused by migration of alkali ions and water molecules into the restricted space of the fine-grained matrix surrounding the dolomite rhomb. This theory argues that expansion is caused when clay, exposed by dedolomitization, attracts and absorbs water. The second theory is that the growth and rearrangement of the dedolomitization reaction products, especially brucite, exerts pressure as it crystallizes. This pressure from the crystallizing products causes expansion (Farny and Kosmatka 1997; Gillott 1995). Ozol (1994) suggests that both theories might be correct, stating that ACR expansion is a result

of a combination of both mechanisms.   The mechanism of ACR expansion according to his theory is caused by a combination of processes, namely:

- migration of alkali ions and water molecules into the restricted space of the calcite-clay matrix surrounding the dolomite rhomb.
- migration of those materials into the dolomite rhomb.
- growth and rearrangement of the de-dolomitization products, especially brucite exerting crystallization pressures, around the outside of the rhombs.

Deng and Tang (1993) however, proposed that dedolomitization caused expansion directly. They proposed that expansion was caused by the crystallization of brucite and calcite in voids. These researchers state that dedolomitization causes a reduction in volume in the beginning. However, after the alkaline solutions penetrate into the interior of the reactive rock and dedolomitization takes place, the fine-grained reaction products of calcite and brucite form and fill voids in the rock. By including the void volume that occurs between these products when formed, an increase in overall volume was found. Deng and Tang (1993) and Qian, et al. (2001) proposed that clay minerals provide a pathway through which H_2O, K^+, Na^+, and OH^- migrate into the interior of the reactive rock.

Regardless of the mechanism, it is known that for the ACR reaction to occur, three criteria must be met. First, the reactive constituent in the reactive aggregate must be in excess of a critical value. Second, there must be sufficient alkali present in the pore solution of the concrete to sustain a reaction. Lastly, sufficient moisture must be available so that the reaction may proceed (Leger 1995).

One important characteristic of the ACR reaction is the fact that it can regenerate and sustain itself. In ACR, calcium hydroxide, produced through cement hydration can

combine with sodium carbonate to form more sodium hydroxide and calcium carbonate.
This reaction regenerates the alkali content of the pore solution, reducing the
concentration of the carbonate ions while providing the reactants to continue the
dedolomitization reaction (Farny and Kosmatka 1997). This reaction is shown in
equation 2-6.

$$NaCO_3 + Ca(OH)_2 \rightarrow NaOH + CaCO_3 \qquad\qquad (2\text{-}6)$$
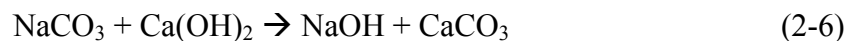
Because of this phenomenon, it is believed by some that ACR can occur even if the pore
solution has a low pH. However, the rate of ACR is affected by the alkalinity of the pore
solution. An increase in ACR potential is associated with an increase in pore solution pH
(Farny and Kosmatka 1997). Others (Ozol 1994) disagrees finding that at a pH lower
than 12, the reaction proceeds slowly, if at all. This same researcher also found that
localized increases in pH resulting from treatment with chemical deicers caused increases
in ACR (Ozol 1994).

Swamy (1994) identified three aggregates with which carbonate reactions
commonly occur. These aggregates are calcitic limestones, dolomitic limestones, or fine-
grained dolomitic limestone aggregates containing interstitial calcite and clay. Farny and
Kosmatka (1997) outline aggregates that have potential for ACR in the following
manner:

- aggregates with a clay content, or insoluble residue content, from 5-25%.
- aggregates with a calcite to dolomite ratio of 1:1.
- aggregates with increasing dolomite volume up to a point at which interlocking
  texture becomes a restraining factor.
- aggregates with discrete dolomite crystals (rhombs) suspended in a clay matrix.

Ozol (1994) also found that the expansion of concrete containing alkali reactive carbonate rocks is promoted by:

- increasing coarse aggregate size
- moisture availability
- higher temperature
- high alkali content of concrete
- high pH of the liquid phase in cement pores
- high proportion of reactive stone in coarse aggregate
- lower concrete strength

Visually, ACR affected pavement is characterized by widespread map cracking that can be more severe at joints. Evidence of joint closing or shoving are possible indicators of expansion in pavement structures. Exudate is common but not always observed with calcium and magnesium silicate hydrate reaction products contributing heavily to the composition of the exudate or "gel". When viewed in the stereo microscope, reactive aggregates in concrete exhibit reaction rims, which are visible alterations of the aggregate surface in contact with cement paste. Care must be exercised to distinguish reaction rims from natural alterations of the aggregate surface such as carbonation. In the petrographic optical microscope or scanning electron microscope (SEM), reaction rims can be examined in detail and reaction product deposits or alterations to the cement paste can also be identified.

Cody et al. (1994), observed similar reaction rims in reactive concrete in Iowa. The rim sequence they reported was unaltered dolomite on the aggregate interior, a dark-colored dolomite reaction rim, a light-colored dolomite reaction rim, a light-colored cement reaction rim in the paste, and dark presumably unaltered cement paste. These

rims are thought to have developed from the dedolomitization reaction, shown in Equation 2-4.

Mineralogically, most ACR aggregates have a characteristic texture. ASTM C 856 states the basic texture as being relatively larger rhombic dolomite crystals in a fine-grained calcite matrix with clay and silt-sized quartz. Substantial amounts of both dolomite and calcite are present.

In order to distinguish reactive from non-reactive aggregate, it is imperative that the aggregate mineralogy and other characteristics, such as porosity, texture, and grain size are known. Milanesi, et al. (1996), stated, XRD studies on rock cylinders showed that dedolomitization occurs at different degrees of intensity, depending on the petrographic characteristics of the rock. Qian, et al. (2001) states that the crystallinity of the individual dolomite crystals may be important in ACR expansion by affecting the dedolomitized rate of aggregate in alkali solutions and is important to determine as well.

In a study done by the Iowa Department of Transportation, durable and non-durable concrete pavements were sampled and examined. The researchers concluded that dedolomitization reactions must be the primary cause (Cody 1994). They reported altered aggregates exhibiting reaction rims, paste alterations of varying degrees with deposition of brucite and calcite rimming reactive dolomite aggregates. The important part of their research is that the composition of their aggregates is far different from the classic composition and fabric discussed in the literature. Cody et. al. reported a reactive dolomite structure with CaO/MgO ratios ranging from 1.483 to 1.775[1]. Also, the rocks they analyzed were not predominately calcite crystals intergrown with dolomite grains.

---

[1] For a 1:1 Ca/Mg stoichiometery, the CaO/MgO ratio is 1.391

The reactive rocks exhibited high porosity without a strong, interlocking crystal fabric. The reactive dolomites contained abundant small, euhedral to subhedral, dolomite crystals as compared to durable aggregates which were primarily coarse, tightly interlocked, dolomite crystals with few euhedral or subhedral outlines. The durable aggregates also had a much lower porosity. Non-durable dolomite aggregates did not contain significantly higher clay concentrations as compared to durable dolomites. Also, Cody et. al. presented evidence that a type of ACR could be induced by calcium and magnesium rich deicing solutions. If supported, their findings would indicate an increased potential for ACR with a much wider array of aggregate type. The research presented by Cody et. al. has not been corroborated by other researchers but should be considered more carefully as more state highway agencies switch to magnesium chloride and calcium chloride deicers.

Alkali-Silica Reaction

Although Michigan uses very little quarried silicate aggregate, a discussion of alkali-silica reaction (ASR) is presented to contrast with the discussion of ACR and provide background for assessment of potential silicate aggregate sources in the future.

Alkali-silica reactivity is a chemical reaction that occurs in the presence of three primary constituents: dissolved alkali within the pore solution of the concrete, aggregates containing accessible amounts of reactive silica, and moisture. ASR can be prevented by careful selection of the concrete constituent materials as it has been found that without one of the three primary constituents, an alkali-silica reaction cannot take place (Stark 1991). The deleterious chemical reaction between the alkali and the reactive silica is two fold. First, the alkali from the pore solution and the silica contained in the aggregate

react to form a gel product. This gel product alone is not deleterious. In the presence of

water, however, this gel product becomes expansive, imbibing water and creating

significant pressure within the paste and aggregates. Preventative measures to curtail

ASR involve screening aggregates and mixing water that may be used in the mix design.

Typically ASR does not occur until years after the concrete has been placed. Methods to

stop ASR are highly experimental (CCAA 1996).

As cement hydrates in the presence of water, calcium and hydroxide ions are

liberated from the calcium silicates (Mindess and Young 1981). This increases the pH of

the pore water to 12 or higher, making it a highly alkaline solution (Gress 1996). The

alkalinity of the pore solution may also be increased by other sources such as fly ash and

certain road salts (ACPA 1995). Over time, the alkalis in the paste pore solution may

react with certain forms of reactive silica contained in the aggregate to form the alkali-

silica gel product. The hydoxyl ions liberated react with the reactive aggregate to

continue production of gel product.

The most reactive forms of reactive aggregate are strained quartz, amorphous

silica, cryptocrystalline quartz, chalcedony, and chert. If water is available, the gel

product will draw it out of the surrounding cement paste causing the gel to swell (Farny

and Kosmatka 1997).   The swelling indicates that the forces of attraction between the

polar water molecules and the alkali-silicate ions from which the gel is composed exceed

the attractive forces between the silicate groups themselves (Gillott 1995). As the gel

expands, it can exert potentially damaging tensile pressures from 4,100 – 11,000 kPa

(600-1600 psi) within the cement matrix (Farny and Kosmatka 1997). These stresses

may also be large enough to cause bond and shear failures between concrete and reinforcement (CCAA 1996).

The penetration of hydroxyl ions into the siliceous aggregates breaks the linkages between the silica tetrahedra. The resultant negatively charged silicate fragments are electrically balanced through interaction with the sodium and potassium ions in the pore solution forming the ASR gel (Harrison 1987).

Factors that affect the rate at which ASR takes place include the amount and type of siliceous materials present, the concentration of alkalis in the pore water solution, and the amount of moisture accessible to the gel product. At higher temperatures, gel expansion is greater but stabilizes earlier (CCAA 1996). There are certain rock types that contain silica that is more reactive. In addition to the rocks named above, the following are known to be potentially reactive: rhyolite, dacite, latite, andesite, tuffs, shale, slate, sandstone, siltstone, quartzite, granites, grano-diorites, and granite gneisses. This list is by no means complete but it implies that a large number of rocks may be reactive and deleterious to concrete (Farny and Kosmatka 1997).

Visible signs of ASR distress include cracks, damp patches, gel exudates, efflorescence, closing of joints, movement, and displacement of members (CCAA 1996). Efflorescence is a deposit of ASR gel found along cracks in concrete. ASR expansion is slow and can cause serviceability problems or exacerbate other deterioration mechanisms (Farny and Kosmatka 1997).

When viewed with a stereo optical microscope or petrographic optical microscope, dark or light reaction rims around coarse aggregates may also be a sign that ASR has occurred. These rims form because the ASR product gel tends to accumulate

around the surface of the reactive aggregate (ACPA 1995). To positively attribute the distress to ASR requires that the presence of the gel product be confirmed. A petrographic analysis as described in ASTM C 856 is recommended for this identification.

Positive identification of ASR also requires that some of the aggregate within the paste be recognized as reactive or potentially reactive. In addition, these aggregates must be partially replaced by the ASR gel product. Coarse aggregate exhibiting internal softening or dissolution, with fracturing that extends to the concrete matrix. is a typical feature in concrete affected by ASR. If only the fine aggregate is reacting, cracking in the matrix may be found that does not affect the coarse aggregates. A network of internal cracks connecting reacted aggregate particles is a strong indication that ASR has occurred.

Deterioration By Deicing Salts

Deicer distress is typically associated with scaling or crazing of the pavement slab surface due to the repeated application of deicing chemicals. Although the exact causes of deicer scaling are not known, it is commonly believed to be primarily a physical attack. Research on deicer scaling has focused on the effects of deicer chemicals on the cement paste fraction of the concrete (Mindess and Young 1981; Pigeon and Plateau 1995). Recent studies suggest that chemical alteration of the cement paste may be occurring, resulting in dissolution of calcium hydroxide, coarsening of the concrete pore system and, potentially, the formation of deleteriously expansive compounds. It has also been speculated that pressure exerted by salt crystallization in voids is a contributing factor (Hansen 1963).

Recent research has focused on possible effects of deicers on concrete cement paste and aggregates. A study conducted for the Iowa DOT investigated the durability of concrete obtained from in-service highways subjected to chloride deicing salts (Cody 1994). Small blocks of concrete cut from 100-mm (4-in) diameter core specimens were subjected to various temperature and saturation regimens while being subjected to soaking in pure distilled water or solutions of magnesium chloride, calcium chloride, or sodium chloride. It is noted that the testing protocol was quite aggressive, with drying temperatures of 60° C and 90° C used in the saturation experiments and low temperatures of -4° C and -70° C used in the freeze-thaw testing.

With regards to the concrete cement paste, the conclusions of the researchers were as follows. Regardless of the in-service performance record, specimens subjected to the harshest temperature, moisture, and chemical environment suffered extensive degradation, characterized by crumbling and fracturing with associated brown discoloration. Magnesium chloride was shown to be the most destructive deicer tested. The mechanism proposed by the researchers is the formation of a non-cementitious magnesium silicate hydrate and the growth of brucite. According to their results, calcium chloride was the next most damaging deicer, which was contributed to the formation of calcium chloroaluminates and pore filling by complex salts produced by interactions between $CaCl_2$, $Ca(OH)_2$, and CO_2. Sodium chloride was found to be relatively benign to the paste. The general conclusion of the study is that magnesium chloride and calcium chloride deicers may create chemical degradation of concrete cement paste through the production of magnesium silicate hydrates or calcium chloroaluminates

The researchers suggest dedolomitization is contributing dissolved magnesium, or brucite, to the cement paste where it is attacking the cement paste, as does magnesium chloride. Therefore, there could be a double effect of ACR – weakening of the aggregate and weakening of the paste.

The study by Cody et. al. (Cody 1994) also examined the effects of deicer chemicals on dolomite coarse aggregate. They determined that magnesium chloride and sodium chloride both had no effect on the non-durable dolomite aggregates previously identified as being reactive in the same study. However, calcium chloride did induce reaction rims in the non-durable dolomite aggregates studied. These new rims showed an increase in magnesium suggesting that the interior, more porous dolomite aggregate underwent dedolomitization enhanced by the calcium chloride. The less porous outer rim areas underwent less dedolomitization appearing magnesium-rich (Cody et al., 1994). To these researchers, this implied that calcium chloride deicers reacted with the aggregate causing dedolomitization. Therefore, ACR may be induced by calcium chloride deicer solutions.

Jang (1993) states that rarely is only one type of degradation at work. Instead, the principal degradation mechanism is supported by the others, accelerating concrete degradation. Jang (1993) states that deicing chemicals will exacerbate alkali-silica reaction, D-cracking, and salt scaling of concrete.

Hudec (1987) reports that chemical deicing salts not only affect cement paste chemically, but also change the freeze-thaw resistance of coarse aggregate. Hudec theorizes that pure water will not normally freeze in the small pore structures typical of some fine-pored rocks. Thus, apparent freeze-thaw durability problems observed among

these rocks is not related to ice formation, but instead to the adsorption of water that occurs within the rock. He observed that deicing salts can make some rocks significantly more sensitive to damage under freeze-thaw cycling and proposes that the salts may contribute to this problem by increasing the amount of adsorbed water within the pore structure through cation adsorption-hydration. Thus, even though the presence of the deicing salts significantly reduces or eliminates freezing of the pore water, freeze-thaw degradation is accelerated through generation of higher osmotic potential resulting in increased pressures. These in turn can lead to fracturing of the aggregate particle and/or aggregate dilation that disrupts the paste.

Another potential effect of chemical deicing salts is increased alkali-silica reactivity. Nixon (1987) reports that salt contamination of concrete, whether through the incorporated aggregate or application of deicing salts, "could be expected to increase the alkalinity of the pore solution and hence the likelihood of damaging alkali silica reaction." The mechanism cited is the combination of sodium chloride with calcium hydroxide and tricalcium aluminate, precipitating calcium chloroaluminate or chloro-sulphoaluminate gel as previously described. He states in cases where sodium chloride is made available through deicer applications, the effect is to produce a zone of reduced alkalinity near the exposed concrete surface, an occurrence consistent with the observations of Muethel (1997).

Crumpton (1989) also reported that the application of salt deicers contributed to the development of ASR and ACR in Kansas, citing the hygroscopic nature of salts that contributed to increased concrete saturation at a given relative humidity. The situation was further aggravated by the increased alkalinity of the pore solution resulting from the

application of deicing salts. This study also found that potassium in the clay fraction of the limestone aggregate had been replaced with sodium from the sodium chloride deicer, altering the degraded illite normally present to a sodium montmorillonite. Crumpton also reported scaling of both paste and aggregate in concrete subjected to cyclic applications of sodium chloride, even without freezing

Summary of Background

Production of durable PCCP requires raw materials that meet the design requirements of the pavement concrete mixture and are suitable for the environment in which the concrete is placed. Distress in PCCP can result from a number of sources that include design/construction-related and materials-related distress. To minimize the occurrence of distresses, proper material selection for the PCC mixture must be done including selection of high quality, durable aggregates. The aggregate properties that most significantly affect durability are:

- Coefficient of thermal expansion.
- Chemical composition.
- Grain size.
- Mineralogy and mineralogical texture.
- Porosity.

Although each of these is determined independently, it is the combination of these characteristics that is important. For example, dolomitic limestones, detectable by compositional analysis, may be ACR reactive if they have a specific combination of mineralogy and mineral texture that is associated with ACR. Large dolomite rhombs distributed in a fine-grained calcite matrix with clay is typical of these potentially ACR reactive dolomitic limestones. Additionally, dolomites with a calcite to dolomite ratio of

approximately 1:1 are potentially reactive. In other research, more common, porous, dolomite textures with fine-grained (typically have a grain size less than 50 microns), poorly interlocking, subhedral to euhedral dolomite crystals have been reported to be reactive. For F-T protection, aggregates should have a small fraction of their pore sizes between 0.5 - 5 microns. Generally, low porosity is preferred and preferably the porosity is not interconnected which would lead to an increase in permeability of the aggregate and of the concrete prepared using that aggregate.

The remainder of this report discusses the measurement of these aggregate properties as they pertain to quarried aggregate sources used for PCCP construction in Michigan. Chapter 3 will present the experimental methods used to determine these values. Chapter 4 will present the results of those measurements. Chapter 5 will provide an analysis of the results including a comparison with known deleterious characteristics identified in this literature review. Chapter 6 will present the conclusions of this research and recommendations for future research.

CHAPTER 3 - EXPERIMENTAL METHODS

Site Descriptions

Thirteen quarries in Michigan, Ohio, and Canada were sampled for this study. It should be noted that the thirteen quarries sampled do not represent all quarries that MDOT uses in producing PCCP. However, the thirteen selected represent the major quarries used. A map showing the physical location of each quarry is shown in Figure 3-1. The symbols used to represent the location of each quarry on the map will be used through out the report to indicate the results from that quarry on plots and graphs.
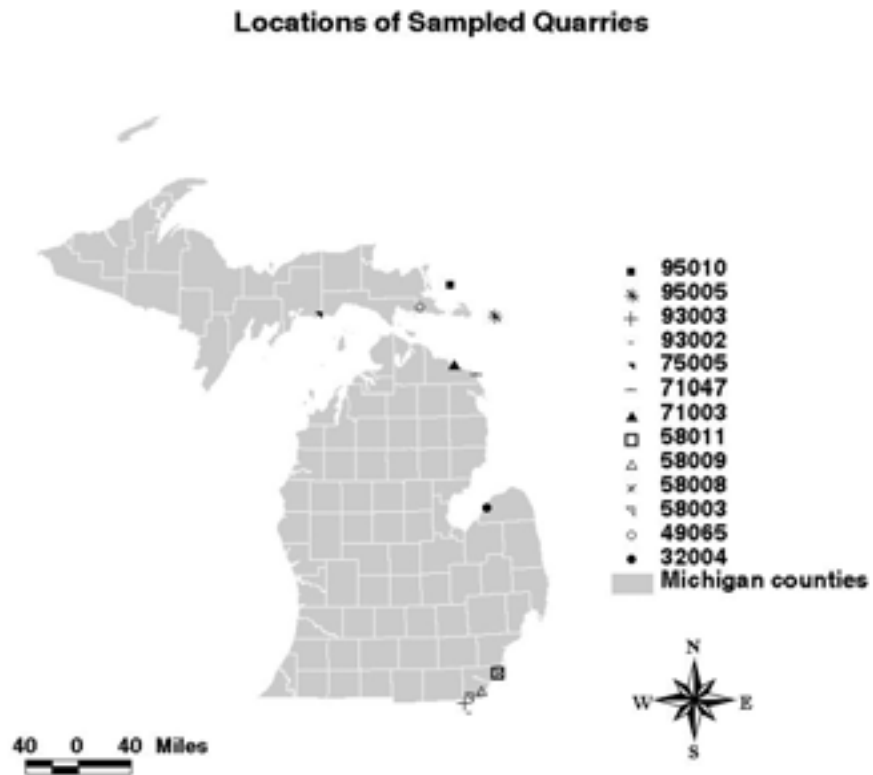

Figure 3-1. A map showing the physical location of each aggregate source studied in this research.

Sampling

Aggregate samples were obtained by MDOT throughout the summer of 2001 with the assistance of MTU. At each quarry, three types of samples were obtained. These included a composite sample of material used to produce a MDOT 6AA gradation, large rocks (approximately 0.5 - 1ft^3), and smaller 2 to 4 in hand specimens from various stockpiles. Each of these samples would be used for different testing purposes

The characteristics used to select the large rocks and hand specimens were color, visual textural differences, and grain size. The large rocks and hand specimens were picked from stockpiles. The goal for this study was to define the spectrum of different rock types present in each of the quarries, but not to quantitatively sample each type. The volume of samples obtained for each rock type does not represent the volume of each rock type present in the deposit being quarried. The large rocks and hand specimens were washed and grouped by sample type using the same characteristics used to select the rocks originally. For the 13 quarries, this resulted in a total of 36 rock types to be analyzed. As part of this process, MDOT representatives obtained samples for CTE testing to be performed at the University of Michigan. These were also large block specimens approximately 0.5 - 1ft^3 in volume.

A 50-gallon drum of 6AA composite sample was obtained from each pit from the 6AA stockpiles. The drum contents were mixed by coning and quartering, split into quarters, and placed in empty barrels for further processing. Taking one quarter, the material was sized using a Gilson sieve. To achieve a 6AA gradation, the sample was sieved into three fractions (+1/2 in, -1/2 in to +No. 4 mesh, and the -No. 4 mesh passing) and then recombined to form a 6AA gradation as shown in Table 3-1. It was desired to

have some +3/4 in material in the gradation but most of the 6AA material sampled had

negligible amounts of +3/4 in material included. Therefore, it was not included in the

final gradation produced.

Table 3-1. Sieve analysis for 6AA samples for lab characterization. The design data
was the target values and the actual values are for the gradations produced.

Size Range	Design Wt Retained (pounds)	Actual Wt Retained (pounds)	Design Cumulative Weight % Retained	Actual Cumulative Weight % Retained
+1 in	1.5	0	0.0	2.5
-1 in +1/2 in	31.5	33.0	55.0	52.5
-1/2 in + 4 mesh	24.6	24.6	41.0	41.0
- 4 mesh	2.4	2.4	4.0	4.0

From mixed and combined 6AA sample, two 60 lbs samples of 6AA were split out with

one being shipped to the University of Michigan for CTE testing and the other to be

processed for analysis at MTU's laboratories.

At MTU, the 60 lbs sample was re-mixed using a riffle splitter and then split into

quarters. One quarter was used for x-ray diffraction analysis, another for microscopy.

The remaining quarters were used for bulk specific gravity (BSG) determination and for a

hand pick sample, respectively. The latter was used to determine the volume fraction of

each rock type in the source.

Laboratory Analysis Methods

The purpose of laboratory analysis was to measure specific properties of the various

aggregate sources, relative to their use in PCCP. These results would form part of the

final database to be developed and help identify aggregate source properties that may

affect PCCP durability. The tests performed are summarized in Table 3-2 indicating

the various aggregate properties measured, the tests employed to make the measurements,

and the specimen form as sampled and as prepared for analysis.

Table 3-2. A summary of the various aggregate properties measured, the tests employed
to make the measurements, and the specimen form as sampled and as prepared for
analysis.

Aggregate Property Measured	Analysis Method	Specimen Form As Sampled	Specimen Form As Prepared for Analysis
CTE	Low Temperature Dilatometer	Large Blocks	Cut Block 5mm x 10mm x 43mm
Grain Size	Petrographic Microscope	Hand Samples	Petrographic Thin Section
Pore Size	Scanning Electron Microscope		Crushed –1 in chips
Mineralogical Composition	X-ray Powder Diffraction	6AA Composite and Hand Samples	Ground Pulverized Powder Approximate Size Distribution of 90% –10μm
Bulk Composition	X-ray Fluorescence Spectroscopy		Ground Pulverized Powder Approximate Size Distribution of 90% –10μm
Bulk Specific Gravity/Abs.	ASTM C 127	6AA Composite	As received

Coefficient of Thermal Expansion

This analysis was conducted at the University of Michigan where a special testing facility

was utilized to determine the dry solid coefficient of thermal expansion (CTE) of

individual aggregate samples. The test set-up consisted of a low-temperature dilatometer,

where the furnace is cooled with liquid nitrogen and heated electrically. This special set-

up was required to obtain continuous measurements of dilation and temperature in the

temperature heating range from 5 to 50º C and the cooling range from 50 to -20º C. The

system response was evaluated against a reference material, in this case structural steel

(A36). This type of steel has an average CTE of 12.0E-06 mm/mm/°C (Hibbeler, 1994).

Two steel samples were tested with an average of 11.5E-6 mm/mm/°C in the temperature range from -20 to 50 °C.

The specimens utilized for CTE determination are 5mm x 10mm rectangular cross sections with a length of 43 mm. These specimens are produced using two lapidary saws with automatically fed vise mechanisms, cross feed mechanism, and oil coolants. Before the specimens are tested, all remaining traces of the saw coolant were removed from the specimen using an ultrasonic cleaner. Once the wet specimens emerge from the bath, they are towel dried and an identification tag is applied. The specimens are then dried at 105 °C for 24 hours. During this drying, water and any remaining oil residue evaporate leaving the uncontaminated specimen.

Grain Size Determination

Petrographic thin sections were made to perform petrographic microscopy and grain size analysis. The billets were impregnated with an epoxy/dye mixture sensitive to UV light to help in identification of voids and other features. The thin sections were then successively ground down by hand in 400, 600, and 1000 grit silicon carbide slurry to a thickness of approximately 30 microns. The last step was to polish the thin sections using a Buehler Ecomet 4 polisher with 9, 6, and 1 micron diamond paste on a tight nylon weave cloth.

To perform the grain size determination, an Olympus BX60 petrographic microscope was used along with an Optronics 3 chip color CCD camera. A Macintosh computer captured images and the public domain National Institutes of Health (NIH) Image 1.62 program was used to analyze the images. Within this program, a macro was written to perform the line intercept analysis used for grain size determination.

Both parallel and perpendicular to bedding thin sections were made. However, after examining both types of thin sections, only the perpendicular thin sections were used in this study. The reason is the perpendicular thin sections include more stratigraphy or structures than the parallel thin sections, which would only include one strata from the specimen.

Both coarse- and fine-grained constituents were seen in thin sections produced from some of the limestone quarries. The coarse-grained constituents consist of fossils and large second generation calcite crystals in vugs, while the fine-grained constituents make up the remaining calcite matrix. Volume percentages of the coarse- and fine-grained constituents were estimated by comparison with published charts to determine the modal percentage of minerals in the rocks. For limestone quarries 75-005 and 71-047, the material exhibited a wide range in grain size between the coarse- and fine-grained constituents and therefore both grain sizes could not be measured at the same magnification. Instead, the line intercepts for the fine-grained matrix were measured with the 20x objective, and the line intercepts for the coarse-grained constituents were measured with the 5x objective. For these two limestone quarries, the summary data presented is a combination of these two separate measurements. For the remaining limestone quarries, (e.g. 32-004 and 71-003) it was possible to collect line intercepts from both the coarse- and fine-grained constituents at the same time with the 10x objective.

Each thin section was placed on the microscope stage and an area was chosen for analysis with the objective lens best suited for the thin section being viewed. A reflected light micrograph was captured as was an image obtained with UV illumination. The UV image was converted to a binary image where all pores appear as white areas and rock

appears as black areas. These two images were overlaid and in the resulting image, air voids were easily seen as white areas. Grain size results were obtained by superimposing a grid of white lines on the digitally processed petrographic micrographs. Intercept lengths of the lines that crossed extinct grains were recorded. Averaging a large number of these intercepts gives the average chord length for the grains, which is used as an estimation of the actual grain size.

Since grain boundaries of extinct grains are more easily seen, only extinct or close to extinct grains were chosen for analysis. A grain had to have two opposite grain boundaries that could be seen on the screen in order to be analyzed. If the grain boundary was blurred, or if there was confusion as to where the grain boundaries were, that grain was not measured.

Three thin sections from each rock type were analyzed. Two micrographs were taken of the same area on a thin section, one at 0° and one at 45° rotation causing different grains go extinct. A minimum of 500 grain intercept lengths were measured for each rock type (167 from each thin section) to get an intercept distribution.

Pore Size Distribution

To determine the average pore volume in the different aggregates, along with the distribution of pore sizes making up that volume, an environmental scanning electron microscope (ESEM) and image analysis were employed. The ESEM used was a FEI XL-40 TMP. The ESEM is computer controlled so the image is acquired digitally, simplifying image acquisition for the digital image analysis. All images acquired for pore size analysis were back scattered electron images (BEI) using a 15 kV accelerating potential.

For each rock type, three thin sections were analyzed using the ESEM as described. These thin sections were prepared separate from the ones used for grain size determination. This was done to provide a thicker section for use in the ESEM. The thin sections were lapped down by hand using 400, 600, and 1000 grit silicon carbide slurry to approximately 1 mm thick. Final polish was with 9, 6, and 1 micron diamond paste on a tight nylon weave cloth.

To process and quantify images obtained from the ESEM, a software program called analySIS Pro was used. Within this program, macros were written to perform the following steps:

- Expand the contrast of each image to a standard value. (This simplifies setting a threshold by making the histogram for each image cover a similar brightness range.)
- Threshold the image to make a binary image where pores are white (255) and holes are black (000).
- Make a binary image based upon the threshold established
- Process each image to identify individual holes (dark areas isolated by white), measure the area fraction of holes, and measure the size and area of each individual hole.
- Compile data in to an Excel spreadsheet format for further processing.

Data compiled from analySIS were further processed using *Mathmatica*, a common mathematical analysis tool. In this step, the pore size distributions were obtained.

Mineralogical Composition

To identify mineral phases in the aggregate analyzed, x-ray diffraction was preformed on all the samples using a Scintag X2 diffractometer and DMSNT-2001 software by Scintag. The sample was scanned from 5° to 90° 2θ to identify all possible minerals. A step size

of 0.02° 2θ with a dwell time of 0.5 seconds per step was used. The tube divergence and scatter slits used were 2 mm and 4 mm respectively, while the detector receiving and scatter slits were 0.2 mm and 0.5 mm respectively. One composite specimen of each sample type and one specimen of the 6AA sample were analyzed. The specimens were finely ground powder and were split from the same samples used for bulk chemical analysis. For further information on the grinding process, refer to the section on Bulk Composition that follows.

Using the software provided, the diffraction patterns obtained were processed to determine the exact location of each diffraction profile in the pattern and it's associated measured intensity. Based upon these measurements, standard databases can be used to identify the possible phases. To determine which phases are represented in an unknown diffraction pattern, the software provides markers to superimpose on the measured diffraction profile to indicate the position and relative intensity of known diffraction profiles in a selected possible phase. This process can be automated but generally misidentifications will occur in this process and manual verification is the only way of ensuring that all phases are correctly identified in the process. Note that although x-ray diffraction can be used to identify clay minerals, detecting those minerals in small quantities is very difficult and requires a significant amount of instrument time, which was beyond the scope of this project.

Mineralogical Texture

To assess the mineralogical texture of the various rocks, the ESEM was used to image fractured pieces from the various rock types sampled. Secondary electron images (SEI) were obtained at a magnification of 1000x using 2kV accelerating potential.

Bulk Specific Gravity and Absorption

Bulk specific gravity was performed on the 6AA material only. As described previously, one-quarter of the starting sample was used for bulk specific gravity and absorption determination. This sample was further split in half and the tests were performed in duplicate and the results averaged. Bulk specific gravity and absorption were determined in accordance with ASTM C 127 *Standard Test Method for Density, Relative Density (Specific Gravity), and Absorption of Coarse Aggregate*.

Bulk Composition

To determine the bulk composition of the aggregate, specimens were sampled and prepared for quantitative x-ray fluoresence spectroscopy (XRF). One quarter of the starting 6AA sample was crushed first with a jaw crusher which was used to reduce the rocks down to approximately -3/4 in. Next, a gyratory crusher was used to further crush the rocks down to approximately -1/4 in. Then a short-head cone crusher was used to reduce the material to -No. 4 mesh. For the final step, a BICO pulverizer ground the rock into fine powder. After each sample was crushed, the crushers were cleaned out with compressed air to eliminate contamination. A splitter was used to divide the resulting powder in half. One half was sent to the Calcite Quarry in Rogers City for x-ray fluorescence analysis, and the other half was used for x-ray diffraction testing.

At Rogers City, the samples were mixed with a binder and pressed into pellets using a ratio of 1.5 grams binder to 15 grams powdered sample. The binder used was methylcellulose from the Aldrich Chemical Company, Inc. This mixture was pulverized for 60 seconds in a puck pulverizer. Twelve grams were weighed from the pulverized mixture and pressed into a 1.25 in pellet. Three pellets were produced from each rock

type sample and each 6AA sample. The pellets were analyzed in an Oxford MDX 1060

XRF spectrometer using XpertEase V2.70 quantitative XRF software. Each pellet was

analyzed for 6 major elements including Mg, Al, Si, S, Fe and Ca. From these elemental

intensities, MgO, Al_2O_3, SiO_2, CaO, and Fe_2O_3, were calculated from their respective

oxide stoichiometry. MgO and CaO were converted to $MgCO_3$ and $CaCO_3$, respectively,

also by stoichiometry

CHAPTER 4 - RESULTS

The results obtained from the analyses described in Chapter 3 have been summarized and included in Volume II of this report titled Materials Characterization Database. These results are in a PDF format that can be easily shared on the WWW. The on-line version of the Materials Characterization Database can be viewed at the following URL: http://www.michigan.gov/documents/RC-1459_121908_7.pdf. The results are presented independently for each quarry. Summaries of pertinent measured values are presented in Chapter 5 of this report.

For each quarry, a general summary is presented including pit name, location, and general geologic information. Next, a summary of general physical properties is presented, including coefficient of thermal expansion (mm/mm/degree C), bulk specific gravity (oven dry), bulk specific gravity (saturated surface dry), apparent specific gravity, percent absorption, average grain intercept length (μm), percent area micro-pores and average micro-pore diameter[2] (μm). A low magnification micrograph of the typical 6AA sample is included along with plots of the average grain intercept length and area percent micro-pores and the raw data used to establish the plots. The next data presented is the composition as determined by x-ray fluorescence and mineral weight percent values computed from x-ray fluorescence. Following this is the same information just described above for the general sample, but instead it is summarized for each rock type identified. For each rock type, these summaries include a description of each type based on differences in color and texture, composition and mineral weight percent values as determined by x-ray fluorescence, x-ray diffraction patterns, petrographic optical microscope and ESEM micrographs, grain intercept length statistics and micro-pore diameter statistics, and the coefficient of thermal expansion.

---

[2] The term micro-pore is used to represent the measurements made on the ESEM, which may not accurately reflect the total porosity but does capture the characteristics of the pores less than 500μm in diameter. Given the high magnification required to image the smaller pores, very large pores or vugs may have been missed in this analysis.

CHAPTER 5 - DATA INTERPRETATION AND DISCUSSION

CTE Determination

As stated in Chapter 2, distress in PCC can be put into the general categories of design/construction- related and materials-related distress. The CTE value of the aggregate is an important characteristic for design/construction-related distress. The CTE values for the sources examined were found to be in excellent agreement with values reported in the literature for each of the dominant rock types. The CTE values of the dolomite sources range from 7.3 to 8.3 x 10^{-6} mm/mm/°C where the expected range from the literature is 7 to 10 x 10^{-6} mm/mm/°C. For limestone sources, the CTE values range from 4.0 to 5.9 x 10^{-6} mm/mm/°C where the expected range is 3.6 to 6.0 x 10^{-6} mm/mm/°C. The gabbro source averaged 6.6 x 10^{-6} mm/mm/°C where the expected range is 5.5 to 8 x 10^{-6} mm/mm/°C. A summary plot of average CTE values for each source is presented in Figure 5-1.

Regarding materials-related distress discussed in Chapter 2, there are four characteristics that can be related to the durability of an aggregate used in the production of PCC. These include chemical composition, mineralogy and mineralogical texture, grain size, and porosity. To aid in comparing the properties listed with measured properties of the aggregates studied, a summary of the results obtained is presented to compare these results with characteristics identified in the literature review.
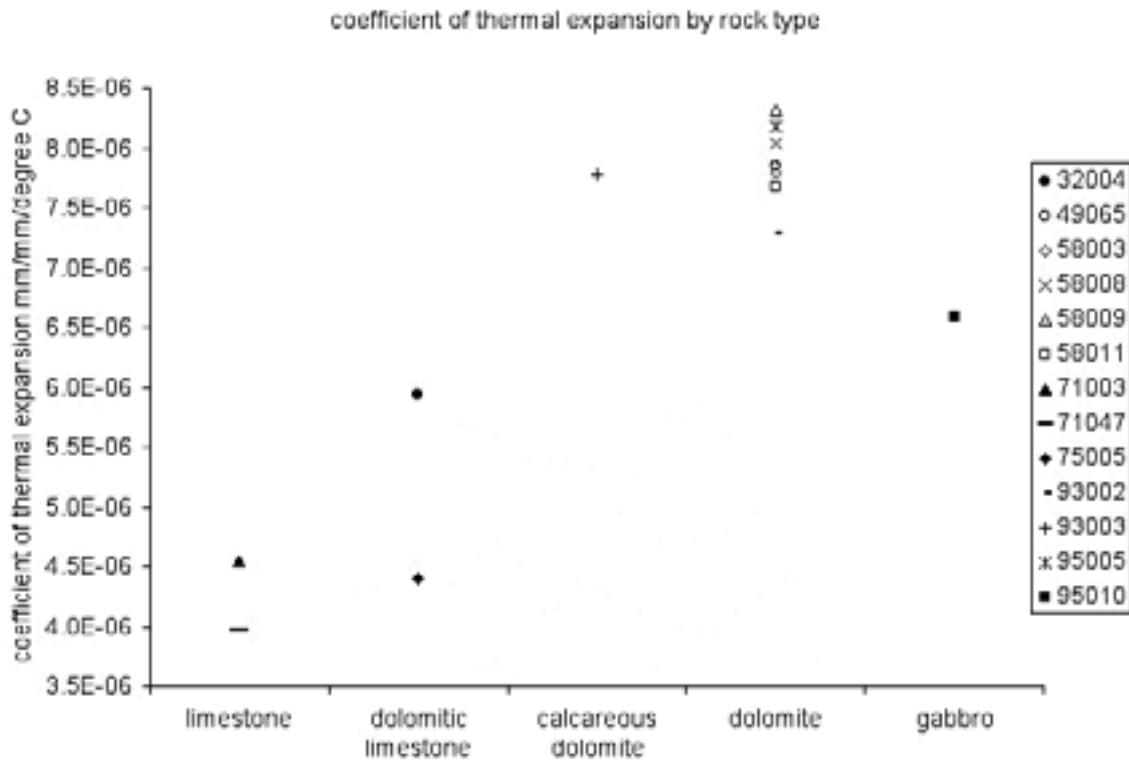
Figure 5-1. Average CTE values for all sources analyzed.

Chemical Composition

Table 5-2 shows the average chemical composition of the carbonate sources examined.

These results are presented in weight percent mineral type, which is recalculated from the

weight percent oxide measurements performed by XRF. Additionally, the CaO to MgO

ratio and Al_2O_3 contents are summarized for discussion. Omitted from Table 5-1 are the

XRF results for pit 95005 which is a gabbro and as such, its chemical composition is not

significant to this analysis.

Table 5-1. Weight percent mineral type recalculated from the weight percent oxide measurements performed by XRF. Also, the CaO to MgO ratio and weight percent Al_2O_3.

MDOT Pit Number	Sample Type	Weight Percent				Dolomite CaO/MgO	Al_2O_3
		Dolomite	Calcite	Pyrite	Other		
32004	6AA	6.30	76.10	0.20	12.70	-	0.40
	Type1	11.50	75.80	0.30	8.20	-	1.40
49065	6AA	98.10	0.50	0.00	0.90	1.40	0.70
	Type1	98.20	0.60	0.00	1.00	1.41	0.10
	Type2	97.80	0.50	0.00	1.20	1.40	0.10
	Type3	98.20	0.20	0.00	1.20	1.40	0.20
58003	6AA	96.20	1.40	0.10	1.60	1.43	0.20
	Type 1	95.20	0.50	0.10	2.70	1.40	0.20
	Type 2	97.50	1.70	0.10	0.80	1.44	0.20
58008	6AA	91.80	2.70	0.30	3.90	1.46	0.20
	Type1	87.70	0.00	0.30	9.60	1.36	0.30
	Type2	97.80	1.50	0.10	0.60	1.43	0.10
	Type3	96.70	1.10	0.30	1.10	1.42	0.40
	Type4	91.20	0.00	0.30	5.40	1.38	0.80
	Type5	65.90	0.00	0.50	28.10	1.19	1.00
58009	6AA	94.40	0.70	0.20	3.30	1.41	0.20
	Type1	95.00	0.70	0.20	2.90	1.41	0.20
	Type2	95.90	1.90	0.10	1.70	1.44	0.20
	Type3	92.50	0.50	0.20	4.80	1.41	0.20
	Type4	91.30	0.00	0.40	5.30	1.38	0.00
58011	6AA	95.10	0.50	0.30	2.50	1.40	0.10
	Type1	91.10	0.00	0.40	4.90	1.38	0.00
	Type2	94.20	0.30	0.20	3.60	1.40	0.30
	Type3	91.20	0.00	0.20	6.50	1.37	0.20
	Type4	91.40	4.80	0.50	0.80	1.53	0.10
	Type5	94.50	0.90	0.60	1.10	1.42	0.20
71003	6AA	2.60	97.00	0.10	0.30	-	1.10
	Type1	3.90	95.60	0.20	0.30	-	0.40
	Type2	2.60	97.40	0.10	0.10	-	0.10
71047	6AA	4.60	94.30	0.10	0.50	-	0.20
	Type1	5.20	93.40	0.10	0.90	-	0.00

Table 5-1 cont. Weight percent mineral type recalculated from the weight percent oxide measurements performed by XRF. Also, the CaO to MgO ratio and weight percent Al_2O_3.

MDOT Pit Number	Sample Type	Weight Percent					
		Dolomite	Calcite	Pyrite	Other	Dolomite CaO/MgO	Al_2O_3
75005	6AA	7.30	90.80	0.10	0.90	-	0.00
	Type1	8.50	89.50	0.10	0.90	-	0.30
	Type2	4.00	94.80	0.10	0.80	-	0.20
	Type3	4.30	94.50	0.10	0.70	-	0.80
93002	6AA	98.30	1.50	0.10	0.20	1.43	0.10
	Type1	97.70	1.20	0.20	0.60	1.43	0.40
	Type2	98.70	1.30	0.00	0.10	1.42	0.30
	Type3	98.70	1.20	0.00	0.10	1.42	0.60
93003	6AA	86.10	9.20	0.20	3.00	1.67	0.10
	Type1	90.30	7.20	0.20	1.60	1.60	0.60
	Type2	89.90	3.10	0.30	4.50	1.48	0.50
	Type3	84.20	14.50	0.10	0.90	1.83	0.20
	Type4	81.60	0.00	0.10	14.10	1.30	0.70
95005	6AA	97.90	0.00	0.10	1.30	1.39	1.20
	Type1	98.40	0.60	0.00	0.50	1.41	0.10
	Type2	97.20	0.00	0.10	1.70	1.38	0.10

None of the aggregate sources analyzed have a chemical composition that by themselves indicates potential problems. For dolomites, the literature indicates that a calcite to dolomite ratio of 1:1 is the threshold for possible reactivity. There were no carbonate rocks analyzed in this study whose calcite to dolomite ratio even marginally approached 1:1. For the dolomites, the CaO/MgO ratio is very near the theoretical composition of dolomite of 1.391 with an average value for the dolomites analyzed being 1.428 and a coefficient of variation (C of V) of 7.1%. The lowest ratio of the sources examined in this study was 1.19 for source 58008, Type 5. A number of the sources have high concentrations of minerals other than calcite and dolomite that is typically quartz. Sources 32004 and 75005 both appear to be dolomitic limestones with 32004 being a

sandy dolomitic limestone. Both sources were examined to assess their mineralogy and texture to confirm they were not similar to the classic ACR reactive aggregates described in Chapter 2.

The best available indicator of clay phases being present is the XRF analysis of alumina (Al_2O_3) in the sources analyzed. Although not absolute, it will give some indication of the possible presence of some clays. In general, none of the sources analyzed contained noticeably high clay contents.

Grain Size

The estimate of grain size for each rock type was determined by petrographic microscopy and image analysis. The mean grain intercept length (MGIL) for each source is used as an estimate of grain size in the rocks examined in this study. For the samples analyzed, these values ranged between approximately 17 and 149 microns. The results of these analyses are shown in Figure 5-2.

The MGIL of a source is determined from the MGILs of the individual rock types within the source and from an estimate of the volume fraction of each type within the 6AA. The MGIL of each rock type was determined by weighting their contribution to the overall MGIL in proportion to their abundance in the 6AA sample. Relative abundance was determined by handpicking the various types from the 6AA sample and determining the weight fraction of each type present. The weight fraction is converted to a volume fraction using the BSG value determined for each rock type.
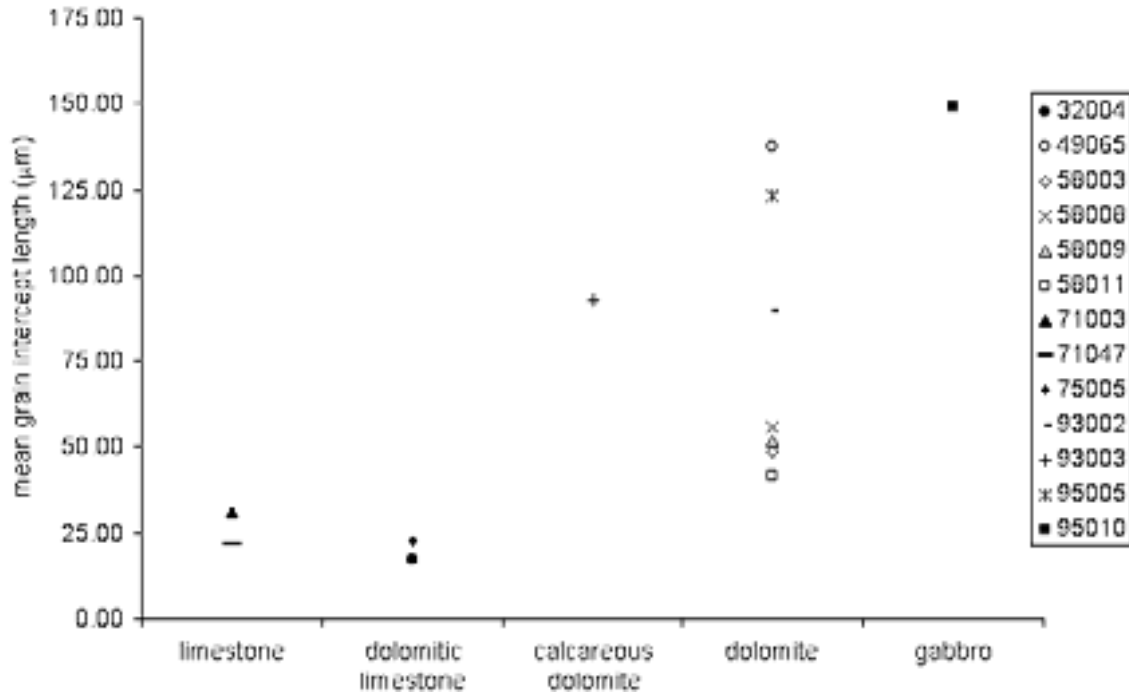
Figure 5-2. Grain size distributions based upon the mean grain intercept analyses performed using petrographic microscopy and image analysis. Each source is grouped with similar rock types on the x-axis.

Fine-grained rocks tend to be more ACR reactive as compared to coarse-grained rocks. The sources with the finest grain size were 32004, 71003, 71047, and 75005 with two of these being limestones and two being dolomitic limestones. Also seen in Figure 5-2, there are a number of sources of dolomite that are fine- to medium-grained including: 58003, 58008, 58009, and 58011 with all having an estimated grain size of approximately 40 to 50 microns. The remaining sources are medium- to coarse-grained with estimated grain sizes ranging from 90 to 137 microns for the carbonates, and 149 microns for 95010.
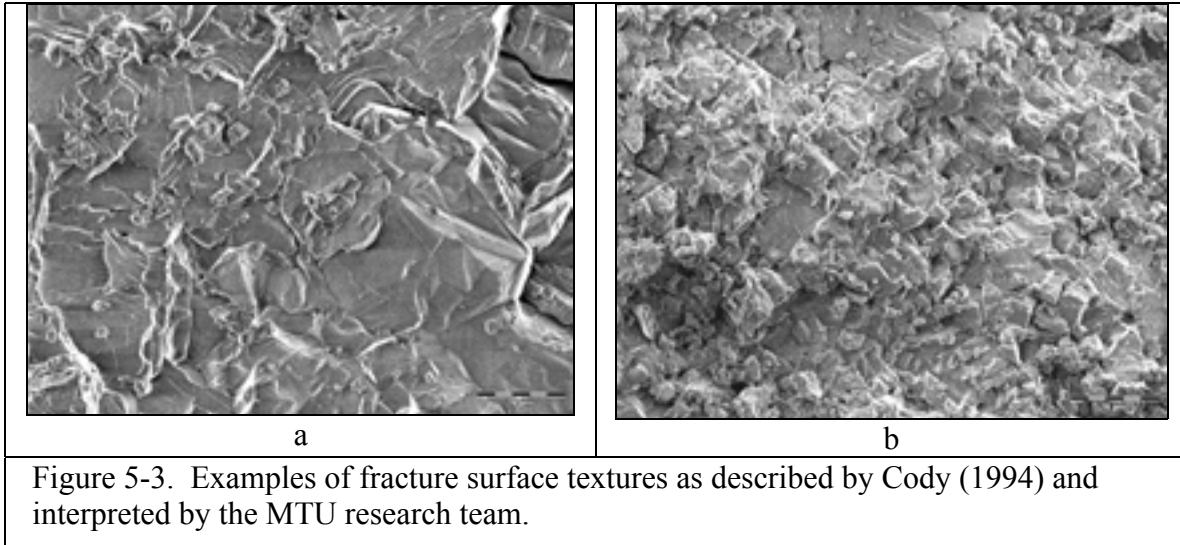
Mineralogy and Texture

The mineralogical data comes from XRF, XRD, and optical petrography. The XRF data was previously presented. The XRD data corroborates the XRF findings and no new phases were identified. Keep in mind that detection of clay minerals is very difficult to achieve by XRD and was not attempted in this study.

Note that none of the aggregates studied exhibited the classic ACR reactive texture discussed in Chapter 2 where dolomite rhombs are dispersed in a fine-grained calcite matrix with clay. This was confirmed by petrographic microscope observation. The closest was 75005 that was a light tan to tan, fine-grained limestone with frequent coarse grained calcite filled vugs and interspersed medium- to coarse-grained dolomite rhombs. It did not have the clay inclusions associated with ACR susceptible aggregates.

Rating the degree of interlocking and grain formation, or texture, is best done by examining the ESEM images of the fracture surface. In general, an absolute assessment is difficult to perform for a given source due to spatial variances in the rock deposit being quarried and the small sample being analyzed. For this study a general classification of texture was made using the work of Cody et. al. (1994) that indicated a more common rock texture as possibly being reactive. In their work, discussed in Chapter 2, they reported durable dolomites were well crystallized with a large grain size and a tightly interlocking often anhedral fabric with low porosity.   The working interpretation of this type of surface is shown in Figure 5-3a.

| a | b |

Figure 5-3. Examples of fracture surface textures as described by Cody (1994) and interpreted by the MTU research team.

In the same study the researchers described non-durable reactive dolomites as predominately fine-grained dolomite with abundant void spaces between poorly-formed dolomite crystals (Cody, 1994). The fine dolomite crystals were 5-50 microns and formed euhedral to subhedral grains poorly interlocked with each other. The working interpretation of this type of surface is shown in Figure 5-3b. For this discussion, the grain sizes of the rocks will be given in ranges where fine is less than 62 microns, medium is 62 - 250 microns, and coarse is greater than 250 microns. Grain sizes may be specified in ranges such as "fine - medium". This indicates the range of particle sizes within the rock. The mean grain intercept length is used as the measure of the grain size for comparison to other rocks in this study.

Two of the finest grained sources, 32004 and 71047 are dolomitic limestones. The fractured specimen surface for 32004 appeared to be more like the durable aggregate fracture surface in Figure 5-3 with moderate to high grain interlocking, and low to moderate porosity. Source 71047 is principally limestone and the fine grain size is typical.

The fine- to medium-grained sources in this study (i.e. 58003, 58008, 58009 and 58011) tended to appear more like the non-durable aggregate fracture surface in Figure 5-3 with euhedral to subhedral grains, which were poorly to moderately interlocked. Based upon visual observation of the specimens, the porosity in these sources were all very high, especially in sources 58008 and 58011. Crystals in the 5-50 micron size range are seen in most of the fine- to medium-grained rocks.

The two Ohio sources, 93002 and 93003 had rock types that appeared more like the durable type in Figure 5.3. Both have visibly high porosity but 93003 has a higher apparent porosity and large calcite grains with interstitial porosity. The medium-grained sources 49065 and 95005 were low in porosity and tightly interlocked anhedral grains. Based upon analysis of the fracture surfaces to assess mineralogical texture, some of the fine- and the fine- to medium-grained rocks exhibited textures that could contribute to poor durability. These include: 58003, 58008, 58009, and 580011. These rock types appear to have texture similar to the non-durable type described by Cody et al. and have a possibility of being ACR reactive.

Porosity

Although porosity can be qualitatively assessed by looking at the fracture surfaces of the various rock types, quantitative determination of porosity requires careful analysis of polished specimens under conditions where topography is not a factor in detecting or measuring the pore sizes. Using the ESEM and digital image analysis, polished specimens from each rock type and the 6AA samples were examined and total pore area and pore size distributions were determined. The results of the total pore area analysis are presented in Figure 5-4 and the average pore size is presented in Figure 5-5. The

value reported for each rock type is the weighted average of the individual rock types

using the same approach as previously described for determining the MGIL.
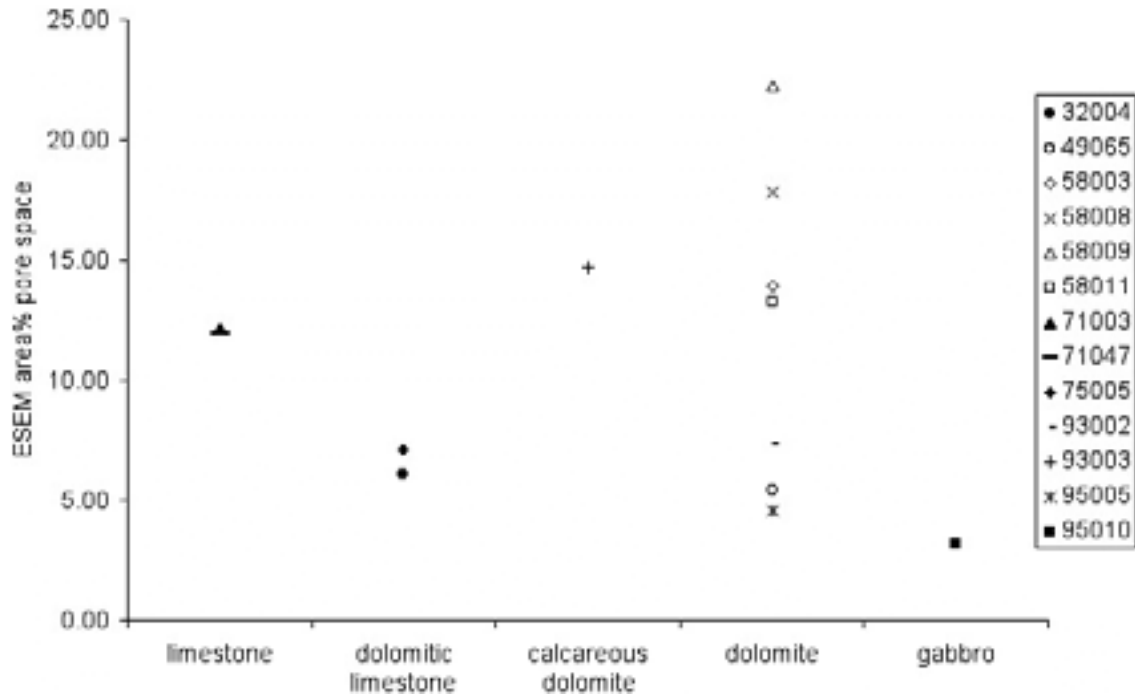
Figure 5-4. Total pore area for each rock type analyzed
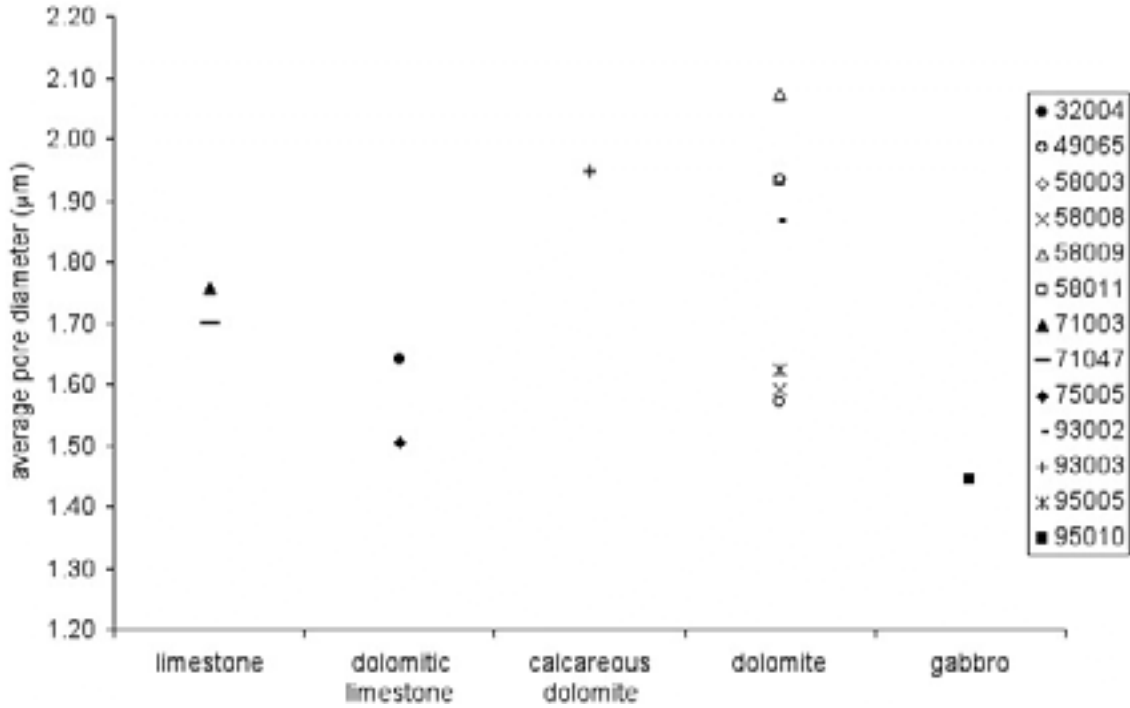
Figure 5-5. Median pore size for each rock type analyzed

Table 5-2. Summary of the percent of all pores with diameters of 1 to 5 microns and total pore area in volume %

MDOT Pit Number	Percent of all Pores with Diameters of 1 to 5 microns	Total Pore Volume Volume %
32004	57.4	6.08
49065	55.0	5.45
58003	37.9	13.88
58008	21.1	17.79
58009	23.6	22.23
58011	24.8	13.26
71003	45.2	12.15
71047	44.9	11.97
75005	65.2	7.08
93002	46.3	7.31
93003	43.3	14.71
95005	58.4	4.57
95010	66.2	3.22

Table 5-2 presents the percentage of all pores with diameters between 1 and 5 microns for each rock type analyzed and total pore volume. The percent of pores with diameters between 1 and 5 microns is chosen because the pixel size for each image was 0.67 microns. Errors in counting the smallest pores will occur when single pixels in an image are considered to represent a pore.

Although an exact threshold for the percent of all pores with diameters of 1 to 5 microns is not established, it can be clearly seen that most of the aggregate sources analyzed have over 40% of their pores occurring in this size class.

A lower total pore volume improves the durability of an aggregate. Four sources; 58003, 58008, 58009, and 58011 have a low percentage of pores in the 1 to 5 micron class, but these sources have the highest total amount of porosity. The pores in 58003, 58008, 58009, and 58011 are larger on average and higher in volume. The larger pores and higher volume of pores must increase the permeability and therefore exposes these types of aggregates to an increased potential for AAR if reactive constituents are present.

With regards to total porosity and its affect on AAR susceptibility or other potential MRDs, no threshold is available in the literature. However, for the sources analyzed, the porosity values fall in to three general categories: 0 to 5 percent, 5 to 10 percent and greater than 10 percent. Those dolomitic aggregates with porosity values in excess of 10 percent offer the highest possibility of being ACR susceptible according to the criterion established by Cody et al. Based on the criterion, the following sources would potentially have the greatest susceptibility to ACR: 58003, 58008, 58009, 58011, and 93003.

Water absorption values for each aggregate source were determined in accordance with ASTM C 127. The results of these tests are presented in Figure 5-6. As a check of the accuracy of the measured porosity values, these measurements were plotted versus the measured pore area and the results are shown in Figure 5-7. As can be seen, a good correlation exists between these two measurements.
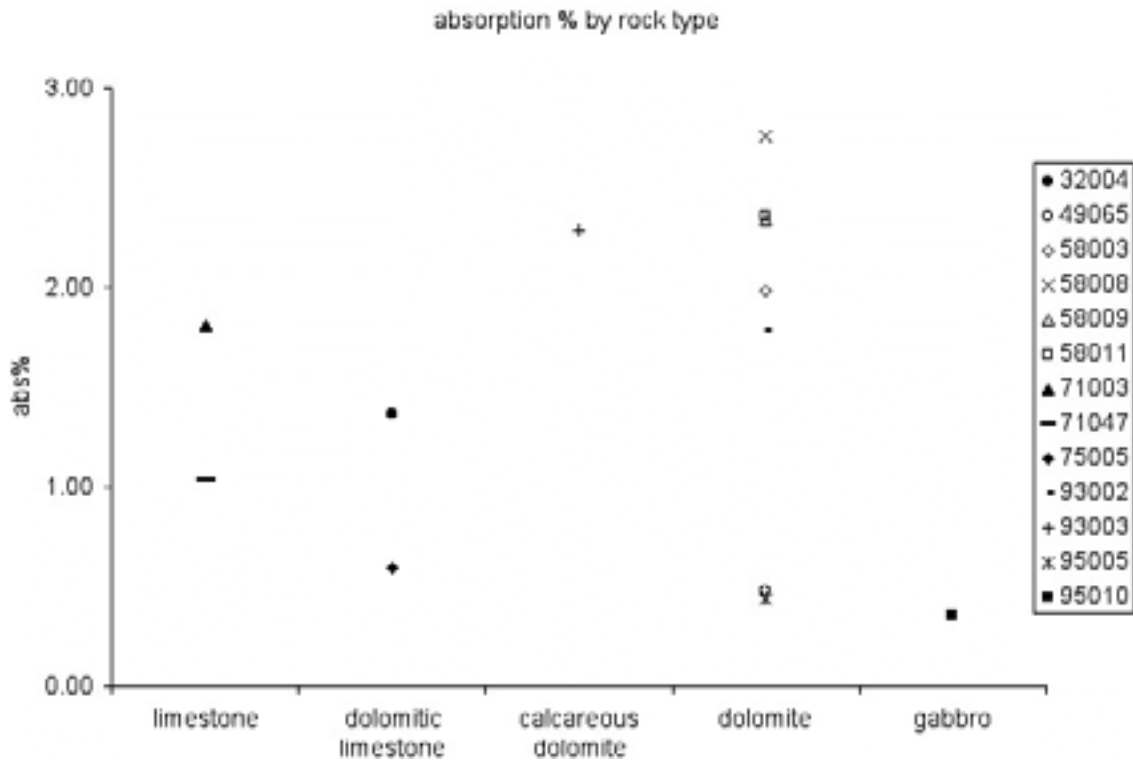
absorption % by rock type

Figure 5-6. Water absorption values for each aggregate source determined in accordance with ASTM C 127
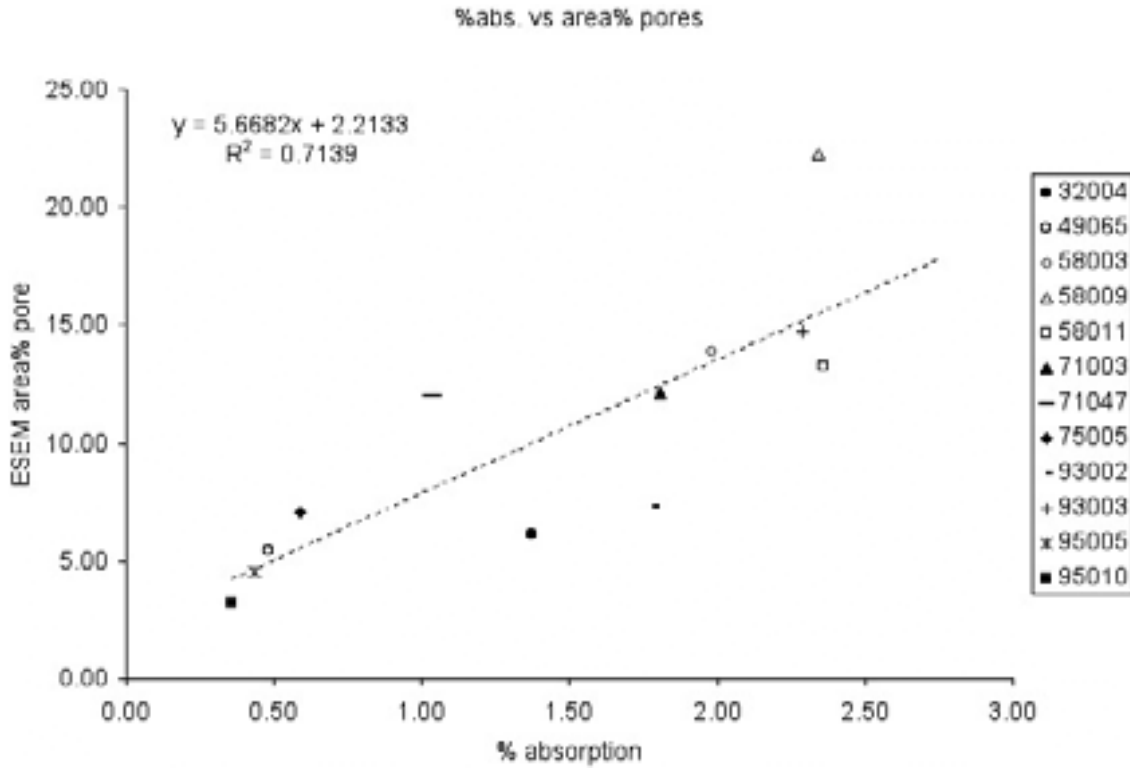
Figure 5-7. Water absorption values for each aggregate source versus measured pore area.

Discussion

Table 5-3 shows the various sources analyzed in the study and a relative rating of each

different characteristic determined for each source. The CTE, chemical composition, and

mineralogy are not included in this table since all the aggregate sources were rated as

excellent according to these characteristics.   Mineralogical texture, grain size, F-T

porosity and ACR potential are included as variation exists in these characteristics

between aggregate sources. The rating system used is a value "1" through "5" with "1"

indicating that the characteristic is normal, or has negligible significance and little to no

influence on durability. A value of "5" indicates the characteristic is highly significant

and almost certainly indicates potential durability issues. A median value of "3"

indicates that in combination with other characteristics, the measured value may be

significant. The average of these values is then used as a relative means of ranking the

various sources with regards to their performance in PCCP with respect to durability.

This ranking is presented in Table 5-4.

Table 5-3 shows that many of the measured properties are consistent with durable

aggregate for use in PCCP. However, it is observed that some microstructural properties

such as texture, grain size, F-T porosity, and ACR potential varied widely over the

sources. In the case of texture, the sources receiving a "3" were the ones that resembled

the non-durable aggregate identified by Cody et al (1994). It must be kept in mind that

these aggregates have not been shown to be non-durable in service conditions, but that

they only possess textural characteristics identified as potentially problematic in

accordance to the work published by Cody et al.

Table 5-3. Relative rating of the different characteristics
determined for each source analyzed in the study.

MDOT Source Number	Texture	Grain Size	F-T Porosity	ACR Potential	Source Average
32004	1	3	2	2	2
49065	1	1	2	2	1.5
58003	3	3	3	3	3
58008	3	3	3	3	3
58009	3	3	3	3	3
58011	3	3	3	3	3
71003	1	3	3	1	2
71047	1	3	3	1	2
75005	1	3	2	2	2
93002	1	2	2	2	1.75
93003	1	2	3	3	2.25
95005	1	1	1	1	1
95010	1	1	1	1	1

Table 5-4. Relative ranking the various sources with regards to their performance in PCCP with respect to durability based upon the total score from the ranking in Table 5-3.

MDOT Pit Number	Source Name	Suitability For Use In PCCP	Source Average
95005	Manitoulin, Canada	1	1
95010	Bruce Mines, Canada	1	1
49065	Cedarville	1	1.5
93002	Maumee, Ohio	2	1.75
32004	Wallace	2	2
71003	Rogers City	2	2
71047	Presque Isle	2	2
75005	Port Inland	2	2
93003	Sylvania, Ohio	2	2.25
58003	Ottawa Lake	3	3
58008	Rockwood	3	3
58009	Denniston Farm	3	3
58011	Newport	3	3

With regards to grain size, a mark of "3" was given to all of the fine-grained sources. ACR potential was ranked for dolimitic aggregates, with those having a total volume of porosity greater than 10 percent being ranked "3", between 5 and 10 percent were ranked "2", and less than 5 percent were ranked "1" to recognize that an increase in permeability results in an increased risk of ACR. All non-dolomitic aggregates were also ranked "1".

The average of all the individual rankings were used as a means of evaluating the aggregate sources and ranking them for potential durability problems when used in PCCP. Note that all of these sources are currently used in the production of PCCP and it is not recommended that the use of any source be curtailed. The ranking is merely an approach to identifying which sources should be studied further to determine if any possible durability issues might result from the use of those sources in PCCP. The

ranking is based upon the thorough characterization performed in this study and offered

as road map for aggregate use in Michigan's highway system.

CHAPTER 6 - CONCLUSIONS

➢ Distress in PCC can be put into the general categories of design/construction- related and materials-related distress.

➢ For design/construction-related distress, one critical characteristic is the CTE value of the aggregate. In this study, CTE values for the sources examined were found to be in excellent agreement with values reported in the literature for each of the dominant rock types and were considered not likely to contribute to design/construction-related distress under normal circumstances.

➢ With regards to materials-related distress, there are four characteristics that can be related to the durability of an aggregate used in the production of PCC. These include chemical composition, grain size, mineralogy, mineralogical texture, and porosity.

- *Chemical Composition* - None of the aggregate sources analyzed have chemical compositions that by themselves indicate potential durability problems. There were no carbonate rocks analyzed in this study whose calcite to dolomite ratio even marginally approached 1:1, and thus no problems would be anticipated based on this characteristic. For the dolomites, the CaO/MgO ratio is very near the theoretical composition.

- *Grain Size* - The estimate of grain size for each rock type was determined by petrographic microscopy and image analysis, with these values ranging between approximately 17 and 149 microns. From the literature, fine-grained rocks tend to be more ACR reactive as compared to coarse-grained rocks. The sources with the finest grain size were 32004, 71003, 71047, and 75005 with two of these being limestones and two being dolomitic limestones. There were a number of sources of dolomite that were fine- to medium-grained including: 58003, 58008, 58009, and 58011 with all having an effective grain size of approximately 40 to 50 microns.

- *Mineralogy* - None of the aggregates studied exhibited the classic ACR reactive texture where dolomite rhombs are dispersed in a fine-grained calcite matrix with clay. The closest was 75005 that was a light tan to tan, fine-grained limestone with frequent coarse-grained calcite filled vugs and interspersed medium- to coarse-grained dolomite rhombs.

- *Mineralogical Texture* - Rating the degree of interlocking and grain formation is best done by examining the ESEM images from the fracture surfaces of each rock type. For this study a general classification of texture was made using the work of Cody et. al. (1994) that indicated a more common rock texture as possibly being reactive. Source 32004 appears to have subhedral grains, moderate to high grain interlocking, and low to moderate porosity. Source 71047 exhibited a typical fine grained limestone structure. The fine- to medium-grained sources in this study all exhibited euhedral to subhedral grains, which were poorly to moderately interlocked. Based upon visual observation of the specimens, the porosity in these sources were all very high, especially in sources 58008 and 58011.Abundant crystals in the 5-50 micron size range are seen in all four of the fine- to medium-grained rocks. The two Ohio sources, 93002 and 93003, had rock types where grains were anhedral with tighter interlocking. Both Ohio sources have visibly high porosity but 93003 has a higher apparent porosity and large calcite grains with interstitial porosity. The coarse-grained sources 49065 and 95005 were low in porosity and had tightly interlocked anhedral grains. Based upon analysis of the fracture surfaces to assess mineralogical texture, a majority of the fine- and the fine- to medium-grained rocks exhibited textures that could contribute to poor durability including: 58003, 58008, 58009, and 58011.

- *Porosity* - Quantitative determination of porosity requires careful analysis of polished specimens under conditions where topography is not a factor in detecting or measuring the pore sizes. Most of the aggregate sources analyzed have the over 40% of their pores occurring in 1 to 5 micron class. The exceptions are sources 58003, 58008, 58009, and 58011. Sources 58003, 58008, 58009, and 58011 have the highest total amount of porosity. For the sources analyzed, the total pore volume values fall in to three general categories: 0 to 5 percent, 5 to 10 percent and greater than 10 percent. As a first approximation, it can be assumed that those with porosity greater than 10 percent offer the highest possibility of being MRD susceptible including: 58003, 58008, 58009, 58011, 71003, 71047, and 93003. Water absorption values for each aggregate source correlated well with the measured volume fraction of pores in each rock type.

➢ A relative rating of each different characteristic determined for each source is provided where "1" indicates that the characteristic has negligible significance and little to no influence on durability. A value of "5" indicates the characteristic is highly significant and almost certainly indicates potential durability issues. A median value of "3" indicates that in combination with other characteristics, the measured value may be significant. The average of these values was used as a relative means of ranking the various sources with regards to their performance in PCCP, with respect to durability.

➢ Sources 58003, 58008, 58009, and 58011 received the poorest ranking and appear to be the sources with the most potential for durability problems. Sources 95005, 95010, and 49065 received the best ranking and appear to be the sources with the least potential for durability problems. Sources 93002, 32004, 71003, 71047, 75005, and 93003 received intermediate rankings. All of these sources are currently used in the production of PCCP and it is not recommended that the use of any source be curtailed.

➢ Based upon the observations and measurements performed in this study, it is recommended that any source with a source average greater than "1.5" be considered as a candidate for future examination, which includes all sources studied except 95005, 95010, and 49065.

CHAPTER 7 - RECOMMENDATIONS FOR FUTURE WORK

Based upon this study, future work is suggested in two areas. First, sources such as 75005, 93003, and 32004 should be sampled more rigorously and a more detailed analysis of their mineralogical structure should be conducted. The basic petrography performed in this study identified these as being possibly of concern but without a more detailed study this can not be confirmed. Second, all sources should be studied for reactivity in concrete by producing concrete using each aggregate and conducting tests for soundness and freeze-thaw resistance in accordance with the proper ASTM and AASHTO procedures. Another research area that is of less importance, but may prove useful in the long run, is to collect a series of cores from each source to determine the amount of each specific rock type and their location within the formation. If a specific rock type were identified as problematic, this information would be useful in avoiding it in the quarry operations or in identifying it in newly developed quarries in the future. Furthermore, in order to better characterize the quarry as a whole, instead of as a sum of specific rock types, it would be better to perform the grain size intercept analysis and the pore size analysis on a true composite sample. A practical approximation of a true composite sample would represent at least one hundred separate particles from the 6AA stockpile material crushed to pass the 3/8" sieve and retained on the No. 4 sieve. Thin sections prepared from such a composite would include hundreds of individual particles, and better characterize the quarry as a whole.

REFERENCES

Addis, B.J., ed. (1986). *Fulton's Concrete Technology.* Portland Cement Insitute, Midrand, South Africa.

American Concrete Pavement Association (ACPA) (1995). *Guide Specification for Concrete Subject to Alkali-Silica Reactions.* Concrete Information. Developed by Alkali-Silica Reactivity/ Pavement Durability Task Group. American Concrete Pavement Association, Skokie, IL. November.

Cement and Concrete Association of Australia (CCAA) (1996). *Alkali Aggregate Reaction: Guidelines on Minimizing the Risk of Damage to Concrete Structures in Australia.* Cement and Concrete Association of Australia and Standards Australia. C&CAA T47. ISBN 0 7337 0469.

Crumpton, C. F., B. J. Smith, and G. P. Jayaprakash (1989). *Salt Weathering of Limestone Aggregate and Concrete Without Freeze-Thaw.* Transportation Research Record 1250. Transportation Research Board. pp. 8-16.

Cody, R. D., Spry, P. G., Cody, A. M., and Gan, G., "The Role of Magnesium in Concrete Deterioration," (1994). Iowa DOT HR-335. Final Report.

Darter, M.I., and Barenberg, E.J. (1977). *Design of Zero-Maintenance Plain Jointed Concrete Pavement*. Report No. FHWA-RD-77-111., Vol. 1.

Deng, M. and Tang M. (1993), "Mechanism of Dedolomitization and Expansion of Dolomititic Rocks," *Cement and Concrete Research*, Vol. 23, pp. 1397-1408.

Farny, James A., and Steven H. Kosmatka (1997). *Diagnosis and Control of Alkali-Aggregate Reactions in Concrete.* Concrete Information Series No. IS413.01T. Portland Cement Association. Skokie, IL. ISBN 0 89312 146 0. 24 pp.

Gress, D. (1997). *Early Distress in Concrete Pavements.* FHWA-SA-97-045, Federal Highway Administration, Washington, DC. January. 53 pp.

Hansen, W., Definis, A., Jensen, E., Byrum, C.R, Mohamed, A.R., Mohr, P., and Grove, G. (1998). *Investigation of Transverse Cracking On Michigan PCC Pavements over Open-Graded Drainage Course.* Final Report submitted to MDOT, University of Michigan.

Harrisson, A., and S. Varma, and N. Winter (1987). *Alkali-Silica Gel Formation at an Early Age Through Solution.* Concrete Durability. Katherine and Bryant Mather International Conference. ACI SP-100. American Concrete Institute, Detroit, MI. pp. 1743-1757.

Huang, Y. H. (1993). *Pavement Analysis and Design*. Prentice Hall, Englewood Cliffs, New Jersey.

Hudec, P. (1987). *Deterioration of Aggregates - The Underlying Causes*. Concrete Durability. Katherine and Bryant Mather International Conference. J.M. Scanlon, Ed. ACI SP-100. pp. 1325-1342.

Jang, J. and I. Iwasaki (1993). Effect of Salt Additives on Concrete Degradation. Report No. MN/RD-93/10. Minnesota Department of Transportation, St. Paul, MN.

Kaneuji, M., D. N. Winslow, and W. L. Dolch (1980). "The Relationship Between an Aggregate's Pore Size Distribution and Its Freeze Thaw Durability in Concrete." *Cement and Concrete Research.* Vol. 10. No. 3. pp. 433-441.

Lane, S. (1994) "Thermal Properties of Aggregates," In *Significance of Tests and Properties of Concrete and Concrete-Making Materials*, Ed. Klieger, P., and Lamond, J.F. ASTM 04-169030-07, pp.438-445.

Leger, P., R. Tinawi, and N. Mounzer (1995). "Numerical Simulation of Concrete Expansion in Concrete Dams Affected by Alkali-Aggregate Reaction: State of the Art." *Canadian Journal of Civil Engineering*. Vol. 22. pp. 692-713.

Leming, M. L. (1996). "Alkali–Silica Reactivity: Mechanisms and Management." *Mining Engineering*. Vol. 48. No. 12. pp. 61-64.

Marks V.J. and Dubberke, W. (1982). *Durability of Concrete and the Iowa Pore Index Test.* Transportation Research Board Record. No. 853. Transportation Research Board. pp.25-30.

Milanesi, C. A., Marfil, S.A., Batic, O. R., and Maiza, P. J. (1996), "The Alkali-Carbonate Reaction and Its Reaction Products An Experience With Argentinean Dolomite Rocks," *Cement and Concrete Research*, Vol. 26, No. 10, pp. 1579-91.

Mindess, S., and J. F. Young (1981). *Concrete*. Prentice-Hall, Inc., Englewood Cliffs, NJ. 671 pp.

Mingshu, T., D. Min, L. Xianghui, and H. Sufen (1994). "Studies on Alkali-Carbonate Reaction." *ACI Materials Journal*. Vol. 91. No. 1. January-February. pp. 26-29.

Misra, S., A. Yamamoto, T. Tsutsumi, and K. Motohashi (1994). "Application of Rapid Chloride Permeability Test to Quality Control of Concrete." *Durability of Concrete*. V. M. Malhotra, Ed. Third International Conference, Nice, France. ACI SP-145. pp. 487-502.

Mobasher, B., and T. M. Mitchell (1988). "Laboratory Experience with the Rapid Chloride Permeability Test." *Permeability of Concrete*. ACI. SP-108. pp. 117-143.

Montgomery, D. A. (1985). *Introduction to Statistical Quality Control.* Wiley and Sons, New York, NY.

Moss, G. M., A. W. Saak, H. M. Jennings, and D. L. Johnson (1997). *Pooled Fund Study of Premature Concrete Pavement Deterioration*. Draft Final Report. Department of Materials Science and Engineering, Northwestern University, Evanston, IL. January 31.

Muethel, R. W. (1997). *Investigation of Calcium Hydroxide Depletion as a Cause of Concrete Pavement Deterioration.* Research Report R-1353. Michigan Department of Transportation Materials and Technology Division. November.

Neville, A. M. (1996). *Properties of Concrete*. John Wiley and Sons, Inc., New York, New York.

Nixon, P., and C. Page (1987). "Pore Solution Chemistry and Alkali Aggregate Reaction." *Concrete Durability*. J.M. Scanlon, Ed. Katherine and Bryant Mather International Conference. ACI SP-100. pp. 1833-1863.

Ozol, M. A. (1994). "Alkali-Carbonate Rock Reactions." *Significance of Tests and Properties of Concrete and Concrete-Making Materials*. STP 169C. Publication Code No. 04-169030-07. American Society for Testing and Materials, Philadelphia, PA. pp. 341-364.

Pigeon, M. (1994). "Frost Resistance, A Critical Look." *Concrete Technology Past, Present, and Future.* V.M. Mohan Malhotra Symposium. ACI. SP-144. pp. 141-157.

Pigeon, M., and R. Plateau (1995). *Durability of Concrete in Cold Climates*. E & FN Spon. ISBN: 0-419-19260-3. 244 pp.

Poblete, M., Salsilli, R., Valenzuela, R., Bull, A., and Spratz, P. (1989). "Field Evaluation of Thermal Deformations in Undoweled PCC Pavement Slabs." *Transportation Research Record*, No. 1207.

Poblete, M., Ceza, P., Espinosa, D.R., Garcia, A., and Gonzalez, J. (1991). "Model of slab cracking for portland cement concrete pavements*." Transportation Research Record*, No. 1307, Transportation Research Board, National Research Council, Washington, DC.

Portland Cement Association (1991). "Design and Construction of Joints for Concrete Highways." *Concrete Paving Technology*, Portland Cement Association.

Qian, G., Deng, M., and Tang, M. (2001), "ACR Expansion of Dolomites with Mosaic Textures," *Magazine of Concrete Research*, Vol. 53, No. 5, pp. 327-336.

Rhodes, C.C. (1949). *Curing Concrete Pavements*. Michigan State Highway Department, Project 42 B-14(2), Report 145.

Schwartz, D. R. (1987). *D-Cracking of Concrete Pavements*. Synthesis of Highway Practice 134. National Cooperative Highway Research Program, Transportation Research Board, Washington, DC.

Shakoor, A., and C. F. Scholer (1985). "Comparison of Aggregate Pore Characteristics as Measured by Mercury Intrusion Porosimeter and Iowa Pore Index Tests." *ACI Journal*. July-August. pp. 453-458.

Spry, P. G., Gan, G., Cody, R. D., and Cody, A. M., "The Formation of Rims on Dolomite Aggregate in Iowa Highway Concrete," Proceedings, 1996 Semisequicentennial Transportation Conference, Iowa 1996, pp. 8-12.

Stark, D. (1974). <u>Field and Laboratory Studies of the Effect of Subbase Type on the Development of D-Cracking</u> (RD021.01P). Portland Cement Association. Reprinted from *Environmental Effects on Concrete*. <u>Highway Research Record</u>. No. 342. Highway Research Record. 1970. pp. 27-34.

Stark, D. (1991). *Handbook for the Identification of Alkali-Silica Reactivity in Highway Structures*. SHRP-C/FR-91-101. Strategic Highway Research Program, Washington, DC.

Sutter, L.L., K.R. Peterson, T.J. Van Dam, K. D. Smith, and M. J. Wade (2002). *Guidelines For Detection, Analysis, And Treatment Of Materials-Related Distress In Concrete Pavements Volume3: Case Studies Using Guidelines*. FHWA-RD-01-165. Federal Highway Administration. Turner-Fairbank Highway Research Center, McLean, VA. March.

Swamy, R. N. (1994). "Alkali-Aggregate Reaction - The Bogeyman of Concrete." *Concrete Technology Past, Present, and Future*. V. M. Mohan Malhotra Symposium. ACI. SP-144. pp. 105-139.

Teller, L.W., and Bosley, H.L. (1930). "The Arlington Curing Experiments." *Public Roads Journal of Highway Research*, USDA, Vol. 10, No. 12.

Teller, L.W., and Sutherland, E.C. (1935). "Observed Effects of Variations in Temperature and Moisture on the Size, Shape, and Stress Resistance of Concrete Pavement Slabs." Public Roads Journal of Highway Research, USDA, Vol. 16, No. 9.

Titus-Glover, L., Owusu-Antwi, E.B., and Darter, M.I. (1999). "Design and Construction of PCC Pavements" FHWA-RD-98-113, U.S. Department of Transportation, Federal Highway Administration.

Van Dam, T.J. (1995). "The Impact of Climate, Load, and Materials on the Performance and Deterioration of GA Airports in Illinois." Ph.D. Thesis, University of Illinois Urbana-Champaign.

Van Dam, T.J., L. L. Sutter, K. D. Smith, M. J. Wade, and K. R. Peterson (2002a). *Guidelines For Detection, Analysis, And Treatment Of Materials-Related Distress In Concrete Pavements - Volume 1: Final Report.* FHWA-RD-01-163. Federal Highway Administration. Turner-Fairbank Highway Research Center, McLean, VA. March.

Van Dam, T.J., L. L. Sutter, K. D. Smith, M. J. Wade, and K. R. Peterson (2002b). *Guidelines For Detection, Analysis, And Treatment Of Materials-Related Distress In Concrete Pavements - Volume 2: Guidelines Description and Use.* FHWA-RD-01-164. Federal Highway Administration. Turner-Fairbank Highway Research Center, McLean, VA. March.

Winslow, D. N. (1994). "The Pore System of Coarse Aggregates." *Significance of Tests and Properties of Concrete and Concrete-Making Materials*. STP 169C. Publication Code No. 04-169030-07. American Society for Testing and Materials. Philadelphia, PA. pp. 429-437.

Zoldners, N.G. (1971). "Thermal Properties of Concrete Under Sustained Elevated Temperatures", Temperature and Concrete" in *Temperature and Concrete*, ACI SP-25, Detroit, MI, pp. 1-31.